

Optimal Classification-based Anomaly Detection with Neural Networks: Theory and Practice

Tian-Yi Zhou^{*†}, Matthew Lau^{*‡}, Jizhou Chen[§], Wenke Lee[¶], Xiaoming Huo^{||}

Abstract

Anomaly detection is an important problem in many application areas, such as network security. Many deep learning methods for unsupervised anomaly detection produce good empirical performance but lack theoretical guarantees. By casting anomaly detection into a binary classification problem, we establish non-asymptotic upper bounds and a convergence rate on the excess risk on rectified linear unit (ReLU) neural networks trained on synthetic anomalies. Our convergence rate on the excess risk matches the minimax optimal rate in the literature. Furthermore, we provide lower and upper bounds on the number of synthetic anomalies that can attain this optimality. For practical implementation, we relax some conditions to improve the search for the empirical risk minimizer, which leads to competitive performance to other classification-based methods for anomaly detection. Overall, our work provides the first theoretical guarantees of unsupervised neural network-based anomaly detectors and empirical insights on how to design them well.

1 Introduction

Anomaly detection (AD) refers to the problem of finding patterns in data that do not conform to expected behavior. AD is extensively used in various applications, such as intrusion detection for cybersecurity [Ambusaidi et al., 2016, Li et al., 2017, Alhajjar et al., 2021], fraud detection [Dorransoro et al., 1997, Zheng et al., 2019], and disease detection [Iakovidis et al., 2018, Lu and Xu, 2018]. Detecting anomalies or outliers in data has been studied in the statistics community as early as the 19th century [Edgeworth, 1887].

In general, AD methods can be categorized into supervised and unsupervised approaches. A supervised approach learns a classification rule using a labeled training sample consisting of labeled normal and anomalous data points. The main challenge lies in generalizing to unknown anomalies and avoiding overfitting to the known labeled anomalies, especially if the problem is set up like a conventional binary classification problem. On the other hand, if only normal/benign data is available during training, then unsupervised AD is used to establish a normal profile from the normal data. In this work, we study the unsupervised AD problem. We focus on a common heuristic in unsupervised AD by artificially generating a new set of data and assigning them as anomalies, which we refer to as “synthetic anomalies”.

Notably, Steinwart et al. [2005] formulate the AD problem as a binary classification problem of “normal” vs. “anomaly”. By transforming the AD problem into a classification task, they were able to establish

[†]H. Milton Stewart School of Industrial and Systems Engineering, Georgia Institute of Technology, tzhou306@gatech.edu

[‡]School of Cybersecurity and Privacy, Georgia Institute of Technology, mlau40@gatech.edu

[§]School of Cybersecurity and Privacy, Georgia Institute of Technology, jzchen@gatech.edu

[¶]School of Cybersecurity and Privacy, Georgia Institute of Technology, wenke@cc.gatech.edu

^{||}H. Milton Stewart School of Industrial and Systems Engineering, Georgia Institute of Technology, huo@gatech.edu

*These authors contributed equally to this work.

the universal consistency of the excess risk (i.e., excess misclassification error) for support vector machines (SVMs).

As neural networks become more ubiquitous due to their strong empirical performance, there has been much work on applying neural networks for AD (e.g., DeepSVDD [Ruff et al., 2018], DAGMM [Zong et al., 2018] and references therein). In particular, Sipple [2020] follows the approach of Steinwart et al. [2005], generating synthetic anomalies but swapping the SVM out with a neural network. Their approach is flexible, which allows them to obtain explainable interpretations [Sipple, 2020] and also potentially incorporate supervision of real anomalies, as in DeepSAD [Ruff et al., 2020] or in Lau et al. [2024b,a]. However, their approach has some limitations. First, by switching the SVM out, the theoretical guarantees for classification-based AD established in Steinwart et al. [2005] no longer hold. Second, they provide no guide on the proportion of synthetic anomalies that should be generated. The number of synthetic anomalies that Sipple [2020] uses is 30-60 times the number of normal training data, but this is empirically tested within a small range. Intuitively, there should be enough synthetic anomalies to allow for an effective supervision signal, but small enough to mitigate contamination of the region of normal data. Third, the sampling approach they adopted does not integrate domain knowledge of the data distribution, especially for data containing one-hot encoded categorical variables. In our paper, we design a theoretically grounded neural network-based approach, aiming to address these concerns and improve their method.

Despite the widespread successes of deep learning in AD practice, scant theoretical results are present to corroborate the observed efficiency and effectiveness of neural networks. Moreover, the number of synthetic anomalies required to guarantee high detection accuracy remains an open question in unsupervised AD. In our work, we present a ReLU neural network method for unsupervised AD and rigorously prove that it approaches optimal classification accuracy with more samples. We then show how to practically implement our proposed method, with our case study on network intrusion detection applications. We outline our main contributions below.

Contributions

In this paper, we consider an unsupervised AD problem where only normal data is available.

1. Based on the important property that anomalies typically occur less frequently than normal/benign data, we characterize the AD problem as a density level set estimation problem. Building upon the framework in [Steinwart et al., 2005], we show that solving a binary classification problem of “normal” vs. “anomaly” can, in turn, solve the level set estimation problem. We further demonstrate that the empirical misclassification error can serve as a viable and computable error metric for AD.
2. To solve this classification problem, we propose a ReLU neural network classifier obtained via empirical risk minimization. During training, we use both the given normal data and synthetic anomalies artificially generated from some probability measure. Under the classic Tsybakov noise condition (Assumption 1) and a mild smoothness assumption on the density function (Equation (11)), we prove that the excess risk of our proposed classifier converges to 0 at a minimax optimal rate (Theorem 1), as the number of normal data increases. To our best knowledge, this is the first result in the AD literature that proves optimality.
3. Furthermore, we provide upper and lower bounds on the number of synthetic anomalies needed to achieve the optimality (Theorem 1). Specifically, optimality holds when the number of synthetic

anomalies does not exceed the number of normal data points, which is far lower (and more data-efficient) than the proposed 30-60 times in [Sipple \[2020\]](#).

4. We implement our proposed method on two real-world datasets on network intrusion detection for cybersecurity, where cyber-attacks are considered anomalies. Our experiments corroborate our theory. We also address some challenges faced during the practical implementation, such as the vanishing gradient and overfitting problems, and show how to facilitate the search for the optimal neural network.
5. Empirically comparing against other existing anomaly detection methods, our proposed method is competitive across all kinds of cyber-attacks and can even perform significantly better than random when other methods fail to.

Our paper is organized as follows. Section 2 formulates AD as a density level set estimation problem, and then shows the equivalent mapping to a binary classification problem via likelihood ratio testing. Section 3 proposes solving the binary classification problem with neural networks via empirical risk minimization. Section 4 presents our main theorem, which proves that the excess risk of the neural network converges at a minimax optimal rate. Section 5 presents the experimental set-up, evaluations and insights on practically implementing the neural network and the optimization procedure. Technical proofs and additional discussions on experiments are relegated to the supplementary materials.

2 Problem Formulation

We first model the unsupervised AD problem as a density level set estimation problem. Then, we formulate a binary classification problem of “normal” vs. “anomaly”. We will show that solving the classification problem can, in turn, solve the level set estimation problem.

2.1 Model Anomaly Detection as Density Level Set Estimation

The estimation of the level set $\{x : h(x) > \rho\}$, where h is an unknown density function of \mathbb{R}^d and $\rho > 0$ is a given constant, has been studied by relatively few researchers and is considered a difficult problem in statistics. Most of the existing methods require strong assumptions on the level set (e.g., the boundary of the level set has a certain smoothness) that are difficult to verify in practice [[Tsybakov, 1997](#), [Jiang, 2017](#), [Cholaquidis et al., 2022](#)]. A notable example is in [Tsybakov \[1997\]](#), where empirical excess masses were used to estimate level sets. The estimation rate deteriorates when $d > 2$ [[Tsybakov, 1997](#), Theorem 4]; thus is not ideal for handling problems in high-dimensional settings.

To interpret anomaly detection as a density level set estimation problem, we leverage the key property that anomalies typically occur less frequently than normal data.

Let \mathcal{X} be a measurable space subset of \mathbb{R}^d , and μ be a known probability measure on \mathcal{X} . Let Q be an unknown data-generating distribution on \mathcal{X} , which has an unknown density h with respect to μ , i.e., $dQ = h d\mu$. We know that the density level set $\{h > \rho\} := \{x : h(x) > \rho\}$, for any $\rho > 0$, describe the concentration of Q .

Due to the low concentration of anomalies relative to normal data, detecting anomalies can be viewed as detecting density level sets for the data-generating density h . Precisely, for a chosen threshold level $\rho > 0$, the set $\{h \leq \rho\}$ detects anomalous data, and equivalently, the set $\{h > \rho\}$ detects normal data.

We study an unsupervised AD problem where only real normal data is available. Throughout this work, we label normal data by $Y = 1$ and anomalies by $Y = -1$. Consider a set of random normal data $T = \{(X_i, 1)\}_{i=1}^n$, where $\{X_i\}_{i=1}^n$ are assumed to be drawn i.i.d. from Q . We know the level set estimation problem aims to estimate the ρ -level set of h (i.e., the set $\{h > \rho\}$) with a chosen $\rho > 0$. We may use the given normal data $\{X_i\}_{i=1}^n$ to construct a function $f_T : \mathcal{X} \rightarrow \mathbb{R}$ for which the set $\{f_T > 0\}$ is an estimate of $\{h > \rho\}$. For any measurable function $f : \mathcal{X} \rightarrow \mathbb{R}$, the following performance measure is widely used to measure how much the sets $\{f > 0\}$ and $\{h > \rho\}$ coincide with one another with respect to the measure μ [Tsybakov, 1997, Ben-David and Lindenbaum, 1997, Halmos, 2013]:

$$S_{\mu, h, \rho}(f) := \mu(\{f > 0\} \Delta \{h > \rho\}), \quad (1)$$

where Δ denotes the symmetric difference. Intuitively, the smaller $S_{\mu, h, \rho}(f)$ is, the more $\{f > 0\}$ coincide with $\{h > \rho\}$. For a function f , $S_{\mu, h, \rho}(f) = 0$ if and only if $\{f > 0\}$ is μ -almost surely identical to $\{h > \rho\}$.

Here, it is important to note that we cannot compute $S_{\mu, h, \rho}(f)$ for all f because $\{h > \rho\}$ is unknown to us. Therefore, we have to estimate it. In statistics, estimating level sets have long been considered a challenging problem. For instance, Steinwart et al. [2005] states that there is no existing method to estimate $S_{\mu, h, \rho}(f)$ from normal training data with guaranteed accuracy in terms of f, μ , and ρ . We provide an intuition of why in Supplement A. Thus, a drawback of modeling unsupervised AD as a level set estimation problem is that there is a lack of an empirical measure of $S_{\mu, h, \rho}(\cdot)$ such that we cannot compare different estimates of $\{h > \rho\}$.

Hence, we want to find an empirical measure that effectively estimates $S_{\mu, h, \rho}(\cdot)$. In the next subsection, we transform density level set estimation to a binary classification problem. More precisely, we show the excess risk of the binary classification problem can be used to estimate $S_{\mu, h, \rho}(\cdot)$. In other words, the excess risk can be considered a surrogate for $S_{\mu, h, \rho}(\cdot)$.

2.2 Density Level Set Estimation as Binary Classification

We formulate a binary classification problem of “normal” ($Y = 1$) vs. “anomaly” ($Y = -1$). Furthermore, we demonstrate the equivalence between solving this classification problem and performing density level set estimation.

Let $\mathcal{Y} = \{-1, 1\}$. Let P be the probability measure on $\mathcal{X} \times \mathcal{Y}$. We proceed to define P based on our normal data distribution Q where $dQ = h d\mu$. We shall first impose an assumption on the marginal distribution on \mathcal{X} . Let $s \in (0, 1)$ denote the proportion of normal data on the domain \mathcal{X} . For a pair of random variable $(X, Y) \in \mathcal{X} \times \mathcal{Y}$, we correspondingly define $P(Y = 1) = s$ and $P(Y = -1) = 1 - s$.

One common approach in unsupervised AD is to artificially generate a separate set of training data and assign them as anomalies, which we refer to as synthetic anomalies [Steinwart et al., 2005, Sipple, 2020]. Following this approach, we generate another training data set $\{X'_i\}_{i=1}^{n'}$ i.i.d. from the known measure μ , and we label them with $Y = -1$ to get $T' = \{(X'_i, -1)\}_{i=1}^{n'}$. Then, we merge the real normal data and synthetic anomalies to form a new training data set $T \cup T' = \{(X_i, 1)\}_{i=1}^n \cup \{(X'_i, -1)\}_{i=1}^{n'}$, enabling the determination of the optimal classification rule for AD. We assume for $Y = 1$, we have $X \sim Q$ and for $Y = -1$, we have $X \sim \mu$. We have the marginal distribution on \mathcal{X} is given by $P_{\mathcal{X}} = sQ + (1 - s)\mu$. For any function f on $\mathcal{X} \times \mathcal{Y}$, we have

$$\int_{\mathcal{X} \times \mathcal{Y}} f(X, Y) dP = s \int_{\mathcal{X}} f(X, 1) dQ + (1 - s) \int_{\mathcal{X}} f(X, -1) d\mu. \quad (2)$$

From (2), we can deduce the conditional class probability function $\eta(X) := P(Y = 1|X)$, which is given by

$$\eta(X) = P(Y = 1|X) = \frac{s \cdot h(X)}{s \cdot h(X) + 1 - s}, \quad \forall X \in \mathcal{X}. \quad (3)$$

The function η is also known as the ‘‘supervisor’’ in binary classification problems. Then, we see that

$$Y|X \sim \text{Bernoulli} \left(P(Y = 1|X) = \frac{s \cdot h(X)}{s \cdot h(X) + 1 - s} \right). \quad (4)$$

Now, we consider a binary classification problem in which the normal class is labeled with $Y = 1$ and the anomaly class is labeled with $Y = -1$. For any classifier $\text{sign}(f)$ induced by a function $f : \mathcal{X} \rightarrow \mathbb{R}$, its misclassification error is given as

$$R(f) = P(\text{sign}(f(X)) \neq Y).$$

The Bayes risk, denoted by R^* , is the smallest possible misclassification error, that is,

$$R^* := \inf_{f: \mathcal{X} \rightarrow \mathbb{R} \text{ measurable}} R(f).$$

A Bayes classifier, denoted by f_c , can minimize the misclassification error (i.e., realizes the Bayes risk). In other words, $R(f_c) = R^*$.

We take $s = \frac{1}{1+\rho}$, where $\rho > 0$ is the predetermined threshold level. It is proven (in [Steinwart et al. \[2005, Theorem 4\]](#)) that for a measurable function $f : \mathcal{X} \rightarrow \mathbb{R}$, $S_{\mu, h, \rho}(f) = 0$ if and only if $R(f) = R^*$. Using our training data set $T \cup T'$, we are interested in finding a function $f_{T, T'}$ such that $R(f_{T, T'}) \rightarrow R^*$ and thus $S_{\mu, h, \rho}(f_n) \rightarrow 0$, as the number of training data grows.

With (4), it is shown in [Steinwart et al. \[2005, Proposition 5\]](#) that the misclassification error can be expressed explicitly as

$$R(f) = sE_Q[\mathbb{1}\{1 \cdot \text{sign}(f(X)) = -1\}] + (1 - s)E_\mu[\mathbb{1}\{-1 \cdot \text{sign}(f(X)) = -1\}] \quad (5)$$

and the Bayes risk

$$R_P^* = sE_Q[\mathbb{1}\{h \leq \rho\}] + (1 - s)E_\mu[\mathbb{1}\{h > \rho\}] \quad (6)$$

can be attained by a Bayes classifier

$$f_c(X) = \mathbb{1}\{h(X) > \rho\} - \mathbb{1}\{h(X) \leq \rho\} = \begin{cases} 1, & h(X) > \rho, \\ -1, & h(X) \leq \rho. \end{cases}$$

When $s = \frac{1}{1+\rho}$, we know $\eta(X) = \frac{s \cdot h(X)}{s \cdot h(X) + 1 - s} > 1/2$ is equivalent to $h(X) > \rho = \frac{1-s}{s}$, and thus

$$f_c(X) = \mathbb{1}\{\eta(X) > 1/2\} - \mathbb{1}\{\eta(X) \leq 1/2\} = \begin{cases} 1, & \eta(X) > 1/2 \\ -1, & \eta(X) \leq 1/2. \end{cases}$$

The Tsybakov noise condition [[Tsybakov, 2004](#)] is considered a standard assumption in binary classification and is widely used to study the quantitative behaviors of classification algorithms. It is stated below.

Assumption 1. For some $c_0 > 0$ and $q \in [0, \infty)$,

$$\mathbb{P}_{\mathcal{X}}(\{X \in \mathcal{X} : |\eta(X) - 1/2| \leq t\}) \leq c_0 t^q, \quad \forall t > 0,$$

where q is often referred to as the **noise exponent**.

Intuitively, this noise condition describes (with parameter $q \in [0, \infty)$) how the η function behaves around the boundary $\{x : \eta(x) = 1/2\}$. Bigger q means there is a bigger jump of η near the boundary $\{x : \eta(x) = 1/2\}$, which is favorable for classification; smaller q (i.e., η close to $1/2$) means there is a plateau behavior near the boundary, which is considered difficult for classification. For the extreme case of hard margin when q is infinity, it implies that η is bounded away from $1/2$.

With the Tsybakov noise condition with noise exponent $q \in [0, \infty)$, a comparison theorem (from [Steinwart et al. \[2005, Theorem 10\]](#)) between the excess risk (i.e., excess misclassification error) $R(\cdot) - R^*$ and $S_{\mu, h, \rho}(\cdot)$ is established for some constant $c > 0$:

$$R(f) - R^* \leq c S_{\mu, h, \rho}(f) \tag{7}$$

and

$$S_{\mu, h, \rho}(f) \leq c (R(f) - R^*)^{\frac{q}{q+1}} \tag{8}$$

for any measurable function $f : \mathcal{X} \rightarrow \mathbb{R}$. Again, our goal is to find a classifier $f_{T, T'}$ based on the training data set $T \cup T'$ such that $f \rightarrow f_c$, or equivalently $R(f) - R^* = R(f) - R(f_c) \rightarrow 0$. Then, using the inequality (8), we know $S_{\mu, h, \rho}(f) \rightarrow 0$ when $R(f) - R^* = R(f) - R(f_c) \rightarrow 0$. Thus, we see that the excess risk $R(\cdot) - R^*$ is a viable error metric for AD.

In the rest of the paper, we will construct a ReLU network classifier such that this classifier can converge to the Bayes classifier f_c .

3 Proposed Method — Empirical Risk Minimization with ReLU Neural Network

We consider merging the two labeled training sets T (real normal data) and T' (synthetic anomalies) as in the previous section, and we use ReLU neural networks to perform the classification task. Our goal here is to specify a hypothesis space, which consists of functions implementable by a specific class of neural networks (i.e., neural networks with specific depths, widths, and parameter values in a specific range) such that the empirical risk minimizer (ERM) in that hypothesis space can learn the Bayes classifier well.

3.1 Mathematical Formulation of ReLU Neural Networks

We consider rectified linear unit (ReLU) feed-forward neural networks that take d -dimensional inputs and produce scalar outputs. To mathematically define the ReLU neural network, we first introduce some notations.

Let $\sigma(x) = \max\{0, x\}$ be the ReLU activation function. When x is a vector, the ReLU activation function is applied element-wise. A ReLU neural network with $L \in \mathbb{N}$ hidden layers and width vector $\mathbf{p} = (p_1, \dots, p_L) \in \mathbb{N}^L$, which indicates the width in each hidden layer, is defined in the following compositional

form:

$$f(X) = f_{\boldsymbol{\theta}}(X) := a \cdot \sigma \left(W^{(L)} \sigma \left(W^{(L-1)} \dots \sigma \left(W^{(1)} X + b^{(1)} \right) \dots + b^{(L-1)} \right) + b^{(L)} \right), \quad (9)$$

where $X \in \mathcal{X} = [0, 1]^d$ is the input, $a \in \mathbb{R}^{p_L}$ is the outer weight, $W^{(i)}$ is a $p_i \times p_{i-1}$ weight matrix with $p_0 = d$, and $b^{(i)} \in \mathbb{R}^{p_i}$ is a bias vector, for $i = 1, \dots, L$. Denote by $\mathbf{W} = \{W^{(i)}\}_{i=1}^L$ the set of all weight matrices, $\mathbf{b} = \{b^{(i)}\}_{i=1}^L$ the set of all bias vectors, and $\boldsymbol{\theta} = \{\mathbf{W}, \mathbf{b}, a\}$ the collection of all trainable parameters in the network.

Let $\|W^{(i)}\|_0$ and $|b^{(i)}|_0$ denote the number of nonzero entries of $W^{(i)}$ and $b^{(i)}$ in the i -th hidden layer. Let $\|\boldsymbol{\theta}\|_{\infty}$ denote the largest absolute value of the parameters in $\boldsymbol{\theta}$, that is,

$$\|\boldsymbol{\theta}\|_{\infty} = \max \left\{ \max_{1 \leq i \leq L} \max_{j,k} |W_{jk}^{(i)}|, \max_{1 \leq i \leq L} \|b^{(i)}\|_{\infty} \right\}.$$

Let $\|\mathbf{p}\|_{\infty}$ denote the maximum number of nodes among all hidden layers. For $L, w, v, K > 0$, we denote the final form of neural network we consider in this paper by

$$\mathcal{F}(L, w, v, K) := \left\{ f \text{ of the form of (9)} : \|\mathbf{p}\|_{\infty} \leq w, \sum_{i=1}^L \left(\|W^{(i)}\|_0 + |b^{(i)}|_0 \right) \leq v, \|\boldsymbol{\theta}\|_{\infty} \leq K \right\}. \quad (10)$$

Specifically, the function class $\mathcal{F}(L, w, v, K)$ consists of ReLU networks with depth L , width vector \mathbf{p} with the maximum number of nodes w , number of network parameters v , and the absolute value of all parameters is bounded by K .

3.2 Target Neural Network Function Class

Here, we aim to specify a hypothesis space (i.e., a neural network function space) such that function(s) in this hypothesis space can learn the Bayes classifier well. To do so, we must impose some constraints on the density function h , thus imposing constraints on the conditional probability function $\eta = \frac{s \cdot h}{s \cdot h + 1 - s}$.

We denote by $C^m(\mathcal{X})$ with $m \in \mathbb{N}$, the space of m -times differentiable functions on \mathcal{X} . For simplicity, we consider the domain $\mathcal{X} = [0, 1]^d$; however, this can be extended to any compact subset of \mathbb{R}^d . For any positive value $\alpha > 0$, let $[\alpha]^- = \lceil \alpha - 1 \rceil \in \mathbb{N} \cup \{0\}$. Let $\boldsymbol{\beta} = (\beta_1, \dots, \beta_d) \in \mathbb{N}_0^d$ be an index vector, where $\mathbb{N}_0 = \mathbb{N} \cup \{0\}$. We define $|\boldsymbol{\beta}| = \beta_1 + \dots + \beta_d$ and $x^{\boldsymbol{\beta}} = x_1^{\beta_1} \dots x_d^{\beta_d}$ for an index vector $\boldsymbol{\beta}$. For a function $f : \mathcal{X} \rightarrow \mathbb{R}$ and an index vector $\boldsymbol{\beta} \in \mathbb{N}_0^d$, let the partial derivative of f with $\boldsymbol{\beta}$ be

$$\partial^{\boldsymbol{\beta}} f = \frac{\partial^{|\boldsymbol{\beta}|} f}{\partial x^{\boldsymbol{\beta}}} = \frac{\partial^{|\boldsymbol{\beta}|} f}{\partial x_1^{\beta_1} \dots \partial x_d^{\beta_d}}.$$

We shall assume the density function

$$h \in \mathcal{H}^{\alpha, r}([0, 1]^d) := \{f \in C^{[\alpha]^-}([0, 1]^d) : \|f\|_{\mathcal{H}^{\alpha}([0, 1]^d)} \leq r\}, \quad (11)$$

which is the closed ball of radius $r > 0$ in the Hölder space of order $\alpha > 0$ w.r.t. the Hölder norm $\|\cdot\|_{\mathcal{H}^{\alpha}([0, 1]^d)}$ given by

$$\|f\|_{\mathcal{H}^{\alpha}([0, 1]^d)} = \sum_{|\boldsymbol{\beta}|_1 \leq [\alpha]^-} \left\{ \|\partial^{\boldsymbol{\beta}} f\|_{C([0, 1]^d)} + \sup_{x \neq y \in [0, 1]^d} \frac{|\partial^{\boldsymbol{\beta}} f(x) - \partial^{\boldsymbol{\beta}} f(y)|}{|x - y|^{\alpha - [\alpha]^-}} \right\}.$$

Note that we can easily prove that $\eta \in \mathcal{H}^{\alpha, r}([0, 1]^d)$ if $h \in \mathcal{H}^{\alpha, r}([0, 1]^d)$.

Our goal is to construct a specific class of neural networks that learn the Bayes classifier $f_c = \text{sign}(\eta - 1/2)$ (i.e., the sign of $\eta - 1/2$). We employ findings from a previous paper [Schmidt-Hieber, 2020], which tells us that a certain class of ReLU networks can approximate any Hölder continuous function well. We relegate the details of this previous result to Supplement B.

Now, we are in a position to define our hypothesis space. In machine learning, the hypothesis space generally refers to the set of all possible models or functions that a learning algorithm can choose from to make predictions based on the given data. In our case, the hypothesis space is a set of functions generated by a specific class of ReLU feedforward network architecture (i.e., ReLU networks with specific depths, widths, sparsity, and parameter values in a specific range). We define such a hypothesis space with the intention that its functions are well-suited to learning the Bayes classifier.

Definition 1 (Hypothesis Space). *Let $\alpha, r > 0$. Assume $\eta \in \mathcal{H}^{\alpha, r}([0, 1]^d)$. For any integers $m \geq 1$ and $N \geq \max\{(\alpha + 1)^d, (r + 1)e^d\}$, we consider ReLU networks*

$$\hat{\eta} \in \mathcal{F}(L^*, w^*, v^*, K^*)$$

with depth

$$L^* = 8 + (m + 5)(1 + \lceil \log_2(\max\{d, \alpha\}) \rceil),$$

maximum number of nodes

$$w^* = 6(d + \lceil \alpha \rceil)N,$$

number of nonzero parameters

$$v^* = 141(d + \alpha + 1)^{3+d}N(m + 6),$$

and all parameters (in absolute value) are bounded by $K^* = 1$. Here, we define a “hard tanh” function $\sigma_\tau : \mathbb{R} \rightarrow [-1, 1]$ for some $0 < \tau \leq 1$ to be the linear combination of four scaled ReLU units given by

$$\sigma_\tau(x) := \sigma\left(\frac{x}{\tau}\right) - \sigma\left(\frac{x}{\tau} - 1\right) - \sigma\left(-\frac{x}{\tau}\right) + \sigma\left(-\frac{x}{\tau} + 1\right) = \begin{cases} 1, & \text{if } x \geq \tau, \\ \frac{x}{\tau}, & \text{if } x \in [-\tau, \tau), \\ -1, & \text{if } x < -\tau. \end{cases} \quad (12)$$

We define our hypothesis space \mathcal{H}_τ with parameter $\tau \in (0, 1]$ to be functions generated by

$$\mathcal{H}_\tau := \text{span}\{\sigma_\tau \circ f : f \in \mathcal{F}(L^*, w^*, v^*, K^*)\}.$$

As a remark, we can see that if τ is close to 0, $\sigma_\tau(x)$ is close to $\text{sign}(x)$. In other words, we use the function σ_τ to approximate the sign function.

3.3 Finding Classifier via Empirical Risk Minimization

In practice, convex loss functions are commonly employed in classification tasks to make computation feasible. Throughout this paper, we adopt the well-known Hinge loss function

$$\phi(t) := \max\{0, 1 - t\}.$$

Learning a neural network classifier with Hinge loss is relatively straightforward owing to the gradient descent algorithm (see, e.g., [Molitor et al., 2021, George et al., 2024]). Also, a well-established and neat comparison theorem from [Zhang, 2004] with respect to Hinge loss facilitates the generalization analysis of neural network classifiers.

Suppose we have a random set of normal data $T = \{(X_i, 1)\}_{i=1}^n$, where $\{X_i\}_{i=1}^n$ are drawn i.i.d. from an unknown distribution Q . Additionally, we generate another i.i.d. training data set $\{X'_i\}_{i=1}^{n'}$ from a known measure μ (e.g., a Uniform distribution on $[0, 1]^d$) and label each sample of it with $Y = -1$.

We merge $T = \{(X_i, 1)\}_{i=1}^n$ and $T' = \{(X'_i, -1)\}_{i=1}^{n'}$ together to form our training data set. For any classifier $f : \mathcal{X} \rightarrow \mathbb{R}$, we define its empirical risk w.r.t. the Hinge loss ϕ as

$$\varepsilon_{T, T'}(f) := \frac{s}{n} \sum_{i=1}^n \phi(1 \cdot \text{sign}(f(X_i))) + \frac{(1-s)}{n'} \sum_{i=1}^{n'} \phi(-1 \cdot \text{sign}(f(X'_i))). \quad (13)$$

Consider the hypothesis space \mathcal{H}_τ defined earlier in Definition 1. We aim to find the empirical risk minimizer (ERM) w.r.t. the Hinge loss ϕ in \mathcal{H}_τ , which is given by

$$\begin{aligned} \hat{f}_{T, T', \phi} &:= \arg \min_{f \in \mathcal{H}_\tau} \varepsilon_{T, T'}(f) \\ &\stackrel{(13)}{=} \arg \min_{f \in \mathcal{H}_\tau} \left\{ \frac{s}{n} \sum_{i=1}^n \phi(1 \cdot \text{sign}(f(X_i))) + \frac{(1-s)}{n'} \sum_{i=1}^{n'} \phi(-1 \cdot \text{sign}(f(X'_i))) \right\}. \end{aligned} \quad (14)$$

In the next section, we prove that the empirical risk minimizer $\hat{f}_{T, T', \phi}$ of our chosen hypothesis space achieves good performance in classification-based anomaly detection. More specifically, we show in Theorem 1 that $R(\hat{f}_{T, T', \phi}) - R^*$, which is equal to $R(\hat{f}_{T, T', \phi}) - R(f_c)$, converges to 0 with an optimal convergence rate in terms of n (i.e., the number of the original unlabeled data).

4 Theoretical Guarantee of ReLU Network for Unsupervised AD

We present our theoretical results in this section.

Consider the hypothesis space \mathcal{H}_τ defined earlier in Definition 1. To show functions in \mathcal{H}_τ can learn the Bayes classifier well, we aim to find a $f \in \mathcal{H}_\tau$ that minimizes the excess risk $R(f) - R^* = R(f) - R(f_c) \geq 0$.

Recall that we assumed the marginal distribution on \mathcal{X} is given by $P_\mathcal{X} = sQ + (1-s)\mu$ for some $s \in (0, 1)$. We also assumed $dQ = hd\mu$, where h is an unknown, Hölder continuous density function. Thus, we know

$$dP_\mathcal{X} = sdQ + (1-s)d\mu = (sh + (1-s))d\mu. \quad (15)$$

For any function $f : \mathcal{X} \rightarrow \mathbb{R}$, its generalization error associated with the Hinge loss ϕ is defined by

$$\begin{aligned}
\varepsilon(f) &= \int_{\mathcal{X}} \int_{\mathcal{Y}} \phi(Yf(X)) dP(Y|X) dP_{\mathcal{X}} \\
&= \int_{\mathcal{X}} [\phi(f(X))P(Y = 1|X) + \phi(-f(X))P(Y = -1|X)] dP_{\mathcal{X}} \\
&\stackrel{(3)}{=} \int_{\mathcal{X}} [\phi(f(X))\eta(X) + \phi(-f(X))(1 - \eta(X))] dP_{\mathcal{X}} \\
&\stackrel{(3),(15)}{=} \int_{\mathcal{X}} [\phi(f(X))sh(X) + \phi(-f(X))(1 - s)] d\mu \\
&\stackrel{::dQ=hd\mu}{=} s \int_{\mathcal{X}} \phi(f(X)) dQ + (1 - s) \int_{\mathcal{X}} \phi(-f(X)) d\mu.
\end{aligned}$$

With the training data set $T \cup T' = \{(X_i, 1)\}_{i=1}^n \cup \{(X'_i, -1)\}_{i=1}^{n'}$, the empirical risk w.r.t. ϕ defined in (13) can be seen as the empirical counterpart of $\varepsilon(f)$.

Recall that we use f_c to denote the Bayes classifier (i.e., the optimal classifier). The well-known Comparison Theorem in classification [Zhang, 2004] states that, for the Hinge loss ϕ and any measurable function $f : \mathcal{X} \rightarrow \mathbb{R}$, there holds

$$\underbrace{R(f) - R(f_c)}_{\text{excess risk}} \leq \underbrace{\varepsilon(f) - \varepsilon(f_c)}_{\text{excess generalization error}}. \quad (16)$$

In other words, we can minimize the excess generalization error (also known as the excess ϕ -error) $\varepsilon(\hat{f}_{T, T', \phi}) - \varepsilon(f_c)$ to, in turn, bound the excess risk $R(\text{sign}(\hat{f}_{T, T', \phi})) - R(f_c)$. To derive convergence rates of the excess generalization error, we assume the Tsybakov noise condition given earlier in Assumption 1. As a recap, Assumption 1 asserts that for some $c_0 > 0$ and $q \in [0, \infty)$, there holds

$$P(\{X \in \mathcal{X} : |\eta(X) - 1/2| \leq t\}) \leq c_0 t^q, \quad \forall t > 0.$$

Below states our main theorem.

Theorem 1. *Let $n \geq 3, d \in \mathbb{N}, \alpha, r > 0, 1/2 \leq s \leq 1$. Consider the hypothesis class \mathcal{H}_τ defined in Definition 1 with $N = \left\lceil \left(\frac{n}{(\log n)^4} \right)^{\frac{d}{d+\alpha(q+2)}} \right\rceil$, $m = \left\lceil \left(1 + \frac{\alpha}{d}\right) \frac{\log N}{\log 2} \right\rceil$, and $\tau = \frac{s}{(1-s)n}$. Let $\hat{f}_{T, T', \phi}$ be the empirical risk minimizer w.r.t. ϕ in \mathcal{H}_τ . Assume the Tsybakov noise condition (Assumption 1) holds for some noise exponent $q \in [0, \infty)$ and constant $c_0 > 0$. Also assume $(\frac{1-s}{s})n \leq n' \leq n$. For any $\delta > 0$, with probability $1 - \delta$, there holds,*

$$R(\text{sign}(\hat{f}_{T, T', \phi})) - R(f_c) \leq \tilde{C} \log\left(\frac{4}{\delta}\right) \left(\frac{(\log n)^4}{n}\right)^{\frac{\alpha(q+1)}{d+\alpha(q+2)}}, \quad (17)$$

where \tilde{C} is a positive constant independent of n or δ .

The proof is in Supplement C. We see that the excess risk bound depends on q , the noise exponent. Theorem 1 tells us that when q increases to ∞ (i.e., stronger noise condition), the convergence rate of the excess risk approaches $\mathcal{O}\left(\frac{(\log n)^4}{n}\right)$. When the number of positive training samples n increases, the excess risk goes to 0. We note that it is proven in [Audibert and Tsybakov, 2007, Kim et al., 2021] that, when $\eta \in \mathcal{H}^\alpha([0, 1]^d)$, the minimax lower bound of the excess risk in binary classification is given by $\mathcal{O}\left(n^{-\frac{\alpha(q+1)}{d+\alpha(q+2)}}\right)$ in the i.i.d. case. So, the convergence rate presented in Theorem 1 matches this optimal one, up to a logarithmic factor. To our knowledge, this is the first result in the AD literature that achieves

the optimal rate.

Moreover, in unsupervised AD, it remains an open question how many synthetic anomalies are necessary to achieve robust detection accuracy. For the first time, we are able to address this question by showing that the optimality of ReLU network classifier is achieved when the number of synthetic anomalies $n' \in \left[\left(\frac{1-s}{s}\right)n, n\right]$. When s is close to 1 (i.e., the majority of data in the domain are normal and $\left(\frac{1-s}{s}\right)$ is close to 0), we only need very few synthetic anomalies for the neural network classifier to perform well. The range of n' stated here aligns with our intuition that there should be enough synthetic anomalies to provide an effective supervision signal, but not too many to contaminate normal data. Note that it is reasonable to assume s to be at least 1/2, because there is typically more normal data than anomalies.

Here, we emphasize the challenge of deriving excess risk bound for this classification problem. The challenge arises due to the non-i.i.d. nature of the data. Our training data $T \cup T' = \{X_i, 1\}_{i=1}^n \cup \{X'_i, -1\}_{i=1}^{n'}$ are non-i.i.d. because T and T' are drawn separately from different distributions. As a result, existing concentration inequalities commonly used in estimation error analysis cannot be applied. We derived novel concentration inequalities in our analysis (e.g., Lemma C.4 and Lemma C.9 in supplementary materials) to accommodate the non-i.i.d. nature of our data.

Next, we apply the comparison theorem stated earlier in (8) to our results in Theorem 1. We recall the performance measure of density level set estimation given in (1)

$$S_{\mu, h, \rho}(f) = \mu(\{f > 0\} \Delta \{h > \rho\}), \quad (18)$$

which measures how much the set $\{f > 0\}$ coincides with $\{h > \rho\}$. The following result presents a high probability upper bound for $S_{\mu, h, \rho}(\text{sign}(\hat{f}_{T, T', \phi}))$.

Theorem 2. *Suppose the assumptions on Theorem 1 hold. Consider the density level set estimation performance measure given in (1). Let $\hat{f}_{T, T', \phi}$ be the empirical risk minimizer w.r.t. ϕ in \mathcal{H}_τ . For any $\delta > 0$, with probability $1 - \delta$, there holds,*

$$S_{\mu, h, \rho}(\text{sign}(\hat{f}_{T, T', \phi})) \leq c \left(\tilde{C} \log \left(\frac{4}{\delta} \right) \right)^{\frac{q}{q+1}} \left(\frac{(\log n)^4}{n} \right)^{\frac{\alpha q}{d + \alpha(q+2)}}, \quad (19)$$

where c is some positive constant, \tilde{C} is a positive constant independent of n or δ .

We can see that as n goes to infinity, $S_{\mu, h, \rho}(\text{sign}(\hat{f}_{T, T', \phi})) \rightarrow 0$, which implies the ReLU network classifier can form a density level set $\{\text{sign}(\hat{f}_{T, T', \phi}) > 0\}$ that converges to our target set $\{h > \rho\}$.

5 Experiments

In the previous section, we have established a non-asymptotic upper bound on excess risk, which demonstrates that the ERM-network can learn the Bayes classifier well. In this section, we conduct a series of real-data experiments to corroborate our main theorem. Specifically, we test our proposed method on network intrusion datasets. We outline the practical steps to find the ERM-network and, based on what we observed during practical implementations, share insights to further improve our model's performance in AD. We also compare the performance of our method with other AD benchmark methods. Furthermore, we performed ablation studies to examine how altering the network architecture, loss function and sampling method affects our model's performance.

In the following, we report our choice of real-world datasets.

5.1 Real-World Datasets for Evaluations

Overview To evaluate the performance of our method and other existing AD methods, we report results from real-world data. We choose to test our methods on network intrusion detection because cyber-attacks are a natural source of non-arbitrary anomalies. We use NSL-KDD [Tavallaee et al., 2009], a common AD benchmark, and Kitsune [Mirsky et al., 2018], a dataset used in NDSS, a top security conference. We detail our selection process in Supplement D.1. The NSL-KDD dataset contains benign (‘normal’) network traffic samples and samples of four different types of cyber-attacks: Denial of Service (DoS), probe, remote access (RA), and privilege escalation (PE). In our experiments, we remove attack samples during training, as per the unsupervised set-up. The data contains three types of features: basic features of a connection (e.g., protocol type, which is a categorical feature), content features within a connection (e.g., number of operations on access control files) and traffic features computed over a time window (e.g., number of connections to the current host in the past two seconds). The Kitsune dataset has a collection of nine sub-datasets, each with benign samples and a different types of cyber-attack sample launched. We select seven attacks (excluding two consistently yielding random performance by all models for brevity): SSDP flood, SSL renegotiation, SYN DoS, active wiretap, ARP MitM, fuzzing, and OS scan. Kitsune has no categorical features, with statistical features on the bandwidth of outbound traffic, the bandwidth of outbound and inbound traffic, the packet rate of outbound traffic and the inter-packet delays of outbound traffic. These datasets are generated with the assumption that the normal data is drawn from the same distribution during the training and testing.

Features In practice, domain experts generate a set of heuristics (and capture features based on these heuristics) to flag out anomalous data, so those attacks that follow these heuristics are easily captured. Here, both datasets opt to use structured and explainable features obtained from feature engineering on the unstructured information of raw network packets. However, there may be unknown “zero-day” attacks that may not follow the heuristics, so the features in the dataset do not directly capture the attack pattern (see Lee and Stolfo [2000], Lee et al. [1999], Lee and Xiang [2001], Perdisci et al. [2009] and Supplement D.1 for more information). Nevertheless, the model can still attempt to use side channels (i.e., side effects) of these attacks for detection. Based on the extracted features, we dichotomize attacks into (1) those more easily detectable attacks where extracted features directly correspond to the attack, and (2) those more difficult-to-detect attacks where extracted features may not directly correspond to the attack. In particular, DoS attacks (DoS in NSL-KDD, SSDP flood/SSL renegotiation/SYN DoS in Kitsune) and probe attacks (in NSL-KDD) are more easily detectable, because they usually involve sending a large number packets and with certain patterns through the network, which can be largely, if not fully, captured by features present in both datasets. Moreover, NSL-KDD also contains features corresponding to information about the payload, which can indicate RA and PE attacks. Here, easier attacks may have conditional probability η closer to 0¹ and RBF kernels may be appropriate to model the data. Meanwhile, the rest of the attacks (in Kitsune) like ARP MitM are mostly dependent on packet content not explicitly captured in the features, so they may not be as separable from normal data (i.e., η closer to 0.5 on average, more distribution overlap between benign and malicious data) and kernels like RBF which encode similarity based on Euclidean distance may not be as appropriate.

¹More precisely, samples x that are ground truth attacks have $\eta(x)$ close to 0. Note that since our test anomaly distribution is not necessary μ , η may not take the original form of (3).

5.2 Excess Risk Convergence Experiments

In this subsection, we conduct experiments using the NSL-KDD dataset to validate our theory. We minimize the empirical risk of a neural network model according to (14) by setting $s = 0.5$ with real benign samples X_i from Q and synthetic anomalies X'_i sampled i.i.d. from a uniform distribution on the domain $\mathcal{X} \subset [0, 1]^d$ (i.e., we consider μ to be the uniform measure on \mathcal{X} as per Steinwart et al. [2005], $d = 119$). We do not have access to the density h to obtain the label $Y|X$ as in (4), but we instead use the ground truth labels provided in the dataset. We normalize each variable to be in $[0, 1]$ and convert categorical variables into one-hot vectors. Here, Q represents the underlying distribution of normal network traffic data of NSL-KDD. We set $n' = n$, that is, the number of benign training samples equals the number of synthetic anomalies in training. Then, we evaluate the neural network model on test data that has real benign samples (assumed to be from Q) and synthetic anomalies sampled i.i.d. from μ . We re-sample training anomalies and re-initialize models thrice to obtain the mean and standard deviation of model performance. We increase the amount of normal data n (and synthetic data n') from 2 to the full training dataset size (around 120k) to test if the accuracy of the learned model converges to an asymptote which should represent the Bayes classifier.

Below, we outline some procedures for implementing our experiments. We then present our experiment results and some discussions.

5.2.1 Practical Implementation

Previously, we defined the target neural network function class in Definition 1. As a quick recap, our target function class consists of ReLU feed-forward networks with a sparsity constraint, and the absolute value of all parameters is bounded by 1. In practice, searching for the empirical risk minimizer in this function class is not straightforward. We proceed to detail some procedures to facilitate the search.

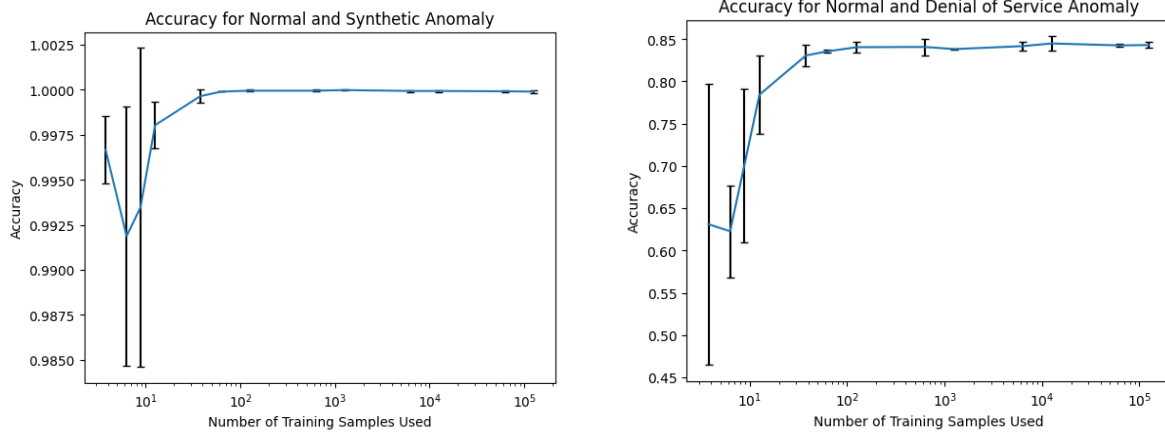
First, we adopt feed-forward neural networks with depth $D := L + 1 = 27$ and width $w = 678$. We experimented with networks of varying depths and widths, and reported results achieved with the best configuration. Second, we find the empirical risk minimizer via gradient descent on hinge loss. In particular, we choose Adam [Kingma and Ba, 2015] as the optimization algorithm because it is known to be generally less sensitive to hyperparameter choice. Additionally, we employ weight decay with Adam to model sparsity constraints that all parameters are bounded by 1 (in absolute value) and constraints on the number of nonzero parameters. We train models until convergence (which, in code, corresponds to 200 epochs with early stopping on the validation loss). Our PyTorch implementation is available in the zipped submission files and is available on GitHub².

5.2.2 Results and Discussion

We show our experiment results in Figure 1. We present the accuracy curve of our ERM-network classifier on the NSD-KDD dataset as the number of training samples increases. In short, the accuracy converges to an asymptote as the number of training samples increases, which corroborates Theorem 1. We give more detailed discussions below on how we address two challenges observed in our experiments to obtain the final result.

First Insight: Size Matters for Vanishing Gradients and Overfitting In our initial attempts, the ERM-network classifier fails to converge across 200 training epochs during training, suggesting vanishing

²<https://github.com/mattlaued/Optimal-Classification-Based-Unsupervised-Anomaly-Detection>



(a) Real normal data and synthetic anomalies (uniformly drawn) with anomaly test ratio of $s = 0.5$. Threshold is uncalibrated.

(b) Real normal data and denial of service attacks (real anomalies) with calibrated threshold. Accuracy curves are similar for other attacks.

Figure 1: Accuracy on NSL-KDD network intrusion dataset, with various test data. Mean and standard deviation across 3 runs plotted. Accuracy converges with more training samples.

gradients. Reducing the depth of the network resolves this issue, but exposes another difficulty of generalization. For relatively deep and wide networks, the validation loss of the models can be decreased to zero without knowledge of its generalizability. Further experiments show that this phenomenon holds even when the size of the network is much smaller than the conditions stated in Theorem 1 and 2. With hinge loss, this behavior is not a surprise — the loss can decrease to zero once the margin is large enough. There are two practical solutions we can adopt to address this overfitting. First, we propose structural risk minimization — reducing the complexity of the model as much as possible while maintaining high validation performance. In addition to weight decay, we also reduce the depth to $D = 3$ and width to $w = 500$. Second, we swap ReLU out for leaky ReLU activations to avoid the dead neuron problem.

Implementing these changes yields models that converge. We plot the accuracy curve (accuracy is one minus misclassification error) in Figure 1a. There is high variance with few training samples n , but we can see that the mean accuracy converges to an asymptote as the number of training data (n and n') increases. This validates our findings in Theorem 1, which states that the excess risk goes to 0 as n increases.

However, we should note that real anomalies likely do not follow μ (the uniform distribution in our experiments). Thus, we also evaluate our method on benign data versus each attack found in the test dataset of NSL-KDD (i.e., real anomalies). We share some findings in the following.

Second Insight: Overfitting to Synthetic Anomalies with Uncalibrated Thresholding Intriguingly, the accuracy of our model on real anomalies decreases with more training data (i.e., higher n) for 2/4 of the attacks. In the original formulation in (1), we mandated that the prediction $f(x) > 0$ classifies x as normal. Although predictions of synthetic anomalies can be very negative and far away from the positively-predicted normal data, the prediction of real anomalies may not be so far away, with many attacks having positive predictions $f(x) > 0$ and wrongly classified as anomalies. From a feature learning perspective, it is possible that the model learns what makes data realistic, similar to what the discriminator in a generative adversarial network (GAN) learns. Hence, since real anomalies have features that make them realistic, the model may not be able to make as accurate predictions compared to synthetic anomalies. In this case, the

model “overfits” to the synthetic anomalies and degrades in performance when facing covariate shift towards real anomalies. An improvement is to choose a threshold $\kappa > 0$ for the classification rule $f(x) > \kappa$ rather than the midpoint $\kappa := 0$. In practice, it is quite common to set such a threshold to allow for β false positives to be more “conservative” to detect more anomalies. We choose $\beta = 5\%$ and calibrate the threshold with the validation data. Often times, κ is well above 0, which reflects the conservativeness of the modeller.

Changing the threshold for classification yields the accuracy curves of all 4 attacks and the synthetic anomalies similar to the convergence rate in (2). We plot one example in Figure 1b. We proceed to use this improved model in the following experiments and refer to it as our theory classifier (TC).

5.3 Evaluation with Anomaly Detection Metrics

In this subsection, we compare our method with other existing AD methods on the NSL-KDD dataset and the Kitsune dataset.

Metrics In AD, evaluations usually defer to metrics other than accuracy and area under the receiver operator characteristic curve (AUROC) because (1) negatives and positives are not necessarily equal in number and (2) predicting wrongly on each of them have different costs. Hence, we use the area under the precision-recall curve (AUPR), also known as average precision, as our main metric (instead of accuracy, as in the previous section). AUPR allows us to measure the separation between the positive (anomaly) and negative (normal) class without a specific threshold, which can be later set by the operator based on desired trade-offs between Type I and II errors. We repeat experiments thrice and report the mean and standard deviation.

Models For each dataset, we compare our theory classifier with other classification-based AD methods, which includes the SVM baseline [Steinwart et al., 2005] and NS-NN [Sipple, 2020]. NS-NN has a similar idea to our approach. The main conceptual differences are that it generates many more synthetic anomalies than our approach (it requires $n' = 30n$), and the synthetic anomalies are drawn from continuous space rather than the support of the distribution. No theoretical guarantee regarding NS-NN is given. We also include results from a random baseline and other unsupervised AD baselines that are not classification-based. The random baseline is calculated in expectation for random guessing, which is equivalent to the fraction of anomalies in the test data. Other unsupervised benchmarks, including OCSVM [Schölkopf et al., 1999], Isolation Forest [Liu et al., 2008] and DeepSVDD [Ruff et al., 2018], may not have the same theoretical guarantees as classification-based approaches, but have worked well empirically. We choose hyperparameters for all models with validation loss when meaningful, and structural risk minimization (as described in Section 5.2.2) otherwise. More details are in Supplement D.2. We report the AUPR of normal data against each cyber-attack in each column of Table 1 for NSL-KDD and Table 2 for Kitsune, where attacks are considered as anomalies.

Overall Results Across all methods, our theory classifier is the best (within 1 standard deviation) on probe and RA attacks and second best on DoS and PE FOR NSL-KDD, and is competitive on 5/7 attacks for Kitsune (SSDP, SYN, Wiretap, ARP MitM, fuzzing). Among the classification-based approaches, our theory classifier has the best AUPR for all attacks in NSL-KDD and 4/7 attacks in Kitsune. Meanwhile, the unsupervised methods have mixed results, with Isolation Forest being the best on 3/4 attacks in NSL-KDD overall but performing worse than OCSVM on Kitsune. Overall, our theory classifier seems to

Table 1: AUPR for KDD, split across attacks in each column. Higher is better, best for each category in bold. Our theory classifier (TC) outperforms the other classification-based approaches SVM and NS-NN, and is second best across all methods.

Model\Attack		DoS	Probe	RA	PE
Random		0.431	0.197	0.007	0.218
Classify	SVM	0.891±0.001	0.838±0.000	0.014±0.000	0.320±0.001
	TC (Ours)	0.909±0.001	0.943±0.002	0.030±0.008	0.401±0.017
	NS-NN	0.517±0.056	0.223±0.040	0.007±0.000	0.218±0.000
Unsup.	OCSVM	0.891±0.000	0.834±0.001	0.018±0.000	0.356±0.000
	IsoF	0.945±0.005	0.941±0.015	0.046±0.039	0.398±0.039
	DeepSVDD	0.824±0.003	0.756±0.003	0.031±0.000	0.492±0.005

Table 2: AUPR for Kitsune, split across attack types. Higher is better, best for each category in bold. Our theory classifier (TC) is best on 4/7 attacks, achieving non-trivial performance for attacks that others struggle to do better than random (ARP MitM and fuzzing).

Model\Attack		SSDP	SSL	SYN	Wiretap	ARP MitM	Fuzzing	OS Scan
Random		0.468	0.077	0.004	0.217	0.761	0.348	0.094
Classify	SVM	1.000±0.000	0.678±0.001	0.060±0.006	0.539±0.005	0.724±0.017	0.322±0.007	0.576±0.000
	TC (Ours)	0.998±0.002	0.565±0.179	0.246±0.002	0.743±0.133	0.851±0.099	0.693±0.139	0.495±0.009
	NS-NN	0.999±0.000	0.649±0.002	0.242±0.000	0.723±0.000	0.801±0.010	0.360±0.000	0.500±0.001
Unsup.	OCSVM	0.999±0.000	0.640±0.000	0.248±0.000	0.571±0.000	0.766±0.000	0.299±0.000	0.500±0.000
	IsoF	0.995±0.007	0.489±0.007	0.229±0.018	0.691±0.013	0.651±0.012	0.254±0.010	0.502±0.001
	DeepSVDD	0.998±0.000	0.640±0.000	0.237±0.001	0.627±0.002	0.620±0.001	0.267±0.006	0.500±0.000

consistently perform above the average. To provide more insight, we proceed to compare our theory classifier to classification-based approaches for attacks that are easy or difficult to detect, based on the features present in the data.

Easily detectable attacks As mentioned in Section 5.1, attacks in NSL-KDD and DoS in Kitsune are easier to detect, because the features present in the dataset directly correspond to the features of the attacks. In other words, the attacks in NSL-KDD and the SSDP flood, SSL renegotiation and SYN flood in Kitsune have conditional probability $\eta(X) := P(Y = 1|X)$ closer to 0 or 1 for the normal and attack data. For these 7 attacks, we see our theory classifier having the best AUPR among classification-based detectors for 5 attacks (DoS, probe, RA, PE and SYN), while SVM has the best AUPR for the other 2 (SSDP and SSL). Our theory classifier has almost perfect AUPR for SSDP attacks, and it has somewhat unstable learning for SSL attacks evidenced by the high standard deviation. Nevertheless, our theory classifier is the overall best for these class of attacks.

Difficult attacks The remaining 4 attacks (wiretap, ARP MitM, fuzzing and OS scan from Kitsune) do not have signals that directly correspond to the features in the dataset. As mentioned in Section 5.1, the implication is that η is closer to 0.5 for the normal data and these attacks, and it is not necessarily the case that data close to each other have similar labels. Hence, kernels that encode such information such as the RBF kernel used for the SVM may not be so informative. For wiretap attacks, we see all methods pick up on side channel information well, with our theory classifier being the best. On the other hand, other methods seem to struggle at ARP MitM and fuzzing attacks, while our theory classifier achieves better-than-random

Table 3: AUPR for KDD, split across attacks in each column. Higher is better. We ablate our theory classifier (TC) across width, depth, activation, loss, sampling proportion and method. Results in red are when the performance is lower than 1 standard deviation from the original TC, while blue is for increased performance. Wider and shallower models are better, while changing leaky ReLU to ReLU has no effect. Our choice of loss and sampling approach also generally improve results — swapping them out reduces the performance of models.

Ablation	Model	DoS	Probe	RA	PE
Original	TC	0.909±0.001	0.943±0.002	0.030±0.008	0.401±0.017
Width w	XL ($w = 1000$)	0.909±0.008	0.939±0.006	0.026±0.000	0.392±0.005
	L ($w = 678$)	0.911±0.006	0.938±0.002	0.029±0.009	0.394±0.023
	S ($w = 335$)	0.907±0.004	0.938±0.005	0.028±0.004	0.393±0.021
	XS ($w = 119$)	0.883±0.013	0.911±0.023	0.021±0.004	0.371±0.051
	XXS ($w = 59$)	0.864±0.015	0.898±0.017	0.022±0.002	0.373±0.025
Depth D	2 layers	0.877±0.008	0.884±0.028	0.015±0.002	0.330±0.022
	4 layers	0.905±0.008	0.941±0.008	0.031±0.008	0.409±0.020
	5 layers	0.884±0.014	0.918±0.013	0.029±0.007	0.396±0.024
	8 layers	0.880±0.029	0.904±0.036	0.027±0.009	0.382±0.034
	11 layers	0.893±0.018	0.911±0.036	0.026±0.005	0.378±0.007
27 layers	0.431±0.000	0.197±0.000	0.007±0.000	0.218±0.000	
Activation	ReLU	0.908±0.002	0.940±0.003	0.030±0.006	0.401±0.015
Loss	Logistic Loss	0.843±0.004	0.729±0.008	0.005±0.000	0.111±0.002
	No Weight Decay	0.887±0.000	0.887±0.003	0.019±0.001	0.311±0.008
Sampling	$n' = 30n$	0.883±0.025	0.860±0.102	0.024±0.011	0.330±0.022
	Continuous	0.878±0.002	0.749±0.002	0.031±0.006	0.447±0.017

AUPR. Our theory classifier has the best result in 3/4 of these attacks.

5.4 Ablations

To understand how each piece of our implementation of the theory classifier contributes to its overall performance, we perform ablations on the NSL-KDD dataset on the width, depth, activation, loss function, weight decay, sampling proportion and sample method. To do this, we switch out each component (while the other components are the same as the original TC) to gather further insights. Our results are in presented Table 3.

Our first observation is that **model expressiveness matters**. We varied the model width between $w \in \{59, 119, 335, 500, 678, 1000\} \approx \{0.5d, d, 3d, 4d, 5.5d, 8.5d\}$, which we nickname as XXS/XS/S/M/L/XL sizes. The performances of the larger models with at least S width ($w \geq 335$) are comparable, but those with XS/XXS width (119/59, where $w \leq d$) lag behind. This validates our intuition in Section 5.2.2, which are based on our theoretical results in Theorem 2, that neural network models should be large enough for expressivity.

However, our second observation is that **gradient signal matters**. Performance remains similar (fluctuates up and down minutely) across 2 to 11 layers, with the 27-layer model having symptoms of vanishing

gradients during training and no meaningful gradients, resulting in random performance. It appears that models that are shallow enough to avoid vanishing gradients are good, while a larger width can compensate for the expressivity lost with shallower models. With a relatively shallow network that provides good gradient signals, swapping out ReLU with leaky ReLU does not have a significant impact on the performance. Meanwhile, changing out the loss from hinge loss to logistic loss seems to significantly affect the gradient signal. In fact, models trained with logistic loss have the greatest performance decline across the changes we make. It is likely that logistic loss, an asymptotic loss, does not go exactly to zero, so our method of choosing hyperparameters with hinge loss does not work well for models trained with logistic loss.

The third observation is that **our theoretical construction is practically helpful**, because the implementation we outline in Section 5.2.1 mostly contributes to the empirical performance. Namely, imposing the sparsity constraint with weight decay and having equal number of synthetic anomalies to normal data ($n' = n$) helps, while sampling anomalies on the support of the distribution yields mixed results. Models trained without weight decay or with 30 times the number of synthetic anomalies ($n' = 30n$, as in Sipple [2020]) have a drop in performance. Meanwhile, sampling anomalies continuously in the ambient space (i.e., a categorical variable encoded as a one-hot vector can now take fractional values) leads to a drop in AUPR for DoS and probe attacks but increase in AUPR for PE attacks, which does not seem to provide conclusive results on this piece yet.

5.5 Limitations and Extensions

As previously mentioned, the performance of models is not only limited by model suitability, but also the informativeness of the features, which determine the separability of the data (i.e., if η is far from 0.5 for the data). In addition, we adopt the classification-based approach because we can theoretically formulate the AD problem for statistical guarantees, but other methods may still work better in practice.

Nevertheless, our ablations show that there is room for improvements to increase the capacity of the model while mitigating vanishing gradients and overfitting. Although validation performance is perfect or close to perfect for all classification-based approaches, the test performance is not. The difference in validation and test performance is due to the difference in the anomaly distributions during training/validation and testing, emphasizing that models need to be designed to generalize well to the covariate shift of the anomaly distribution. This is a complementary and promising next step to our improvement on NS-NN to model the AD problem with theoretical guarantees.

6 Related Works

6.1 Unsupervised Anomaly Detection

In this work, we explored the modeling aspect of classification-based approaches for unsupervised anomaly detection. To do this, we viewed unsupervised anomaly detection as a density level detection problem, which is common in the literature [Davenport et al., 2006, Jiang, 2017, Scott and Nowak, 2006]. Other works also generate synthetic data to use a classifier for anomaly detection, such as using RIPPER (inductive decision tree learner) in Fan et al. [2001], random forest and neural networks in Sipple [2020] and SVM in Steinwart et al. [2005]. Steinwart et al. [2005] is the only work proving excess risk convergence.

Apart from the binary classification-based approaches, there are many other approaches to unsupervised anomaly detection. There are some methods inspired by minimum volume set estimation, which is tightly

connected to density level set estimation, such as kernel-based OCSVM/SVDD [Schölkopf et al., 1999, Tax and Duin, 2004] and its neural network variant DeepSVDD [Ruff et al., 2018] (and its extensions [Zhang et al., 2024, Pang et al., 2019]). Other methods leverage higher level ideas, such as mining relationships with auxiliary tasks [Bergman and Hoshen, 2020] and contrastive learning [Cai and Fan, 2022, Qiu et al., 2021, Shenkar and Wolf, 2022]. The advantage of our approach is that we have a systematic modeling approach that allows us to quantify the expected performance in terms of statistical guarantees.

Complementary work has been done to explore the efficacy of sampling methods for classification-based approaches. In particular, sampling around the manifold of normal data for more realistic synthetic anomalies has been explored by Davenport et al. [2006] and Fan et al. [2001] for tabular data and by Hendrycks et al. [2019] for images. These methods can be integrated into our approach and are not mutually exclusive to our work.

6.2 Theoretical Works related to Anomaly Detection

Our work is built on Steinwart et al. [2005], where we swap out their SVM with a neural network. Blanchard et al. [2010] does AD in the transductive fashion, where test data is available together with training data. This setting is more informative than the unsupervised setting, but limits a model from being deployed in production. Neyman-Pearson classification is similar in weighting Type I and II errors differently, and can be used along with optimal likelihood ratio tests [Gu et al., 2008, Hoballah and Varshney, 1989], but still assumes a known distribution of both normal and anomaly classes (e.g., Tong et al. [2016]) which is not available in unsupervised AD.

7 Conclusion

We develop the first theoretically grounded neural network-based approach for unsupervised anomaly detection. Transforming anomaly detection into a binary classification problem via density level set estimation, we train neural networks with supervision from synthetic anomalies. Given a range of the proportion of synthetic anomalies, we prove non-asymptotic upper bounds and optimal convergence rates on the excess risk. Our real-world experiments provide insights on how to more effectively find the empirical risk minimizer. Our experiments demonstrate that our approach improves the current classification-based anomaly detectors, especially for difficult-to-detect attacks, while being theoretically grounded.

Fundings

This work has been supported by the National Science Foundation (NSF) AI Institute for Agent-based Cyber Threat Intelligence and Operation (ACTION) under the NSF grant number IIS-2229876. Huo and Zhou are also partially sponsored by the A. Russell Chandler III Professorship at Georgia Institute of Technology.

References

KDD Cup 1999 Data. UCI Machine Learning Repository, October 1999. URL <https://kdd.ics.uci.edu/databases/kddcup99/kddcup99.html>.

- Elie Alhajjar, Paul Maxwell, and Nathaniel Bastian. Adversarial machine learning in network intrusion detection systems. *Expert Systems with Applications*, 186:115782, 2021.
- Mohammed A Ambusaidi, Xiangjian He, Priyadarsi Nanda, and Zhiyuan Tan. Building an intrusion detection system using a filter-based feature selection algorithm. *IEEE Transactions on Computers*, 65(10):2986–2998, 2016.
- Jean-Yves Audibert and Alexandre B Tsybakov. Fast learning rates for plug-in classifiers. *The Annals of Statistics*, pages 608–633, 2007.
- Shai Ben-David and Michael Lindenbaum. Learning distributions by their density levels: A paradigm for learning without a teacher. *Journal of Computer and System Sciences*, 55(1):171–182, 1997.
- Liron Bergman and Yedid Hoshen. Classification-based anomaly detection for general data. In *International Conference on Learning Representations (ICLR)*, 2020.
- Gilles Blanchard, Gyemin Lee, and Clayton Scott. Semi-supervised novelty detection. *Journal of Machine Learning Research*, 11(99):2973–3009, 2010.
- Jinyu Cai and Jicong Fan. Perturbation learning based anomaly detection. In *Advances in Neural Information Processing Systems (NeurIPS)*, 2022.
- Alejandro Cholaquidis, Ricardo Fraiman, and Leonardo Moreno. Level set and density estimation on manifolds. *Journal of Multivariate Analysis*, 189:104925, 2022.
- Mark A Davenport, Richard G Baraniuk, and Clayton D Scott. Learning minimum volume sets with support vector machines. In *2006 16th IEEE Signal Processing Society Workshop on Machine Learning for Signal Processing*, pages 301–306. IEEE, 2006.
- Jose R Dorronsoro, Francisco Ginel, C Sgnchez, and Carlos S Cruz. Neural fraud detection in credit card operations. *IEEE Transactions on Neural Networks*, 8(4):827–834, 1997.
- Francis Ysidro Edgeworth. Xli. on discordant observations. *The London, Edinburgh, and Dublin Philosophical Magazine and Journal of Science*, 23(143):364–375, 1887.
- Wei Fan, M. Miller, S.J. Stolfo, Wenke Lee, and P.K. Chan. Using artificial anomalies to detect unknown and known network intrusions. In *Proceedings 2001 IEEE International Conference on Data Mining*, pages 123–130, 2001.
- Erin George, Michael Murray, William Swartworth, and Deanna Needell. Training shallow ReLU networks on noisy data using hinge loss: When do we overfit and is it benign? *Advances in Neural Information Processing Systems (NeurIPS)*, 36, 2024.
- Guofei Gu, Alvaro A. Cárdenas, and Wenke Lee. Principled reasoning and practical applications of alert fusion in intrusion detection systems. In *Proceedings of the 2008 ACM Symposium on Information, Computer and Communications Security*. Association for Computing Machinery, 2008.
- H. Guvenir, Burak Acar, Haldun Muderrisoglu, and R. Quinlan. Arrhythmia. UCI Machine Learning Repository, 1998. DOI: <https://doi.org/10.24432/C5BS32>.
- Paul R Halmos. *Measure Theory*, volume 18, pages 17–18. Springer, 2013.

- Dan Hendrycks, Mantas Mazeika, and Thomas Dietterich. Deep anomaly detection with outlier exposure. In *International Conference on Learning Representations (ICLR)*, 2019.
- I.Y. Hoballah and P.K. Varshney. Distributed bayesian signal detection. *IEEE Transactions on Information Theory*, 35(5):995–1000, 1989.
- Dimitris K Iakovidis, Spiros V Georgakopoulos, Michael Vasilakakis, Anastasios Koulaouzidis, and Vassilis P Plagianakos. Detecting and locating gastrointestinal anomalies using deep learning and iterative cluster unification. *IEEE Transactions on Medical Imaging*, 37(10):2196–2210, 2018.
- Heinrich Jiang. Density level set estimation on manifolds with DBSCAN. In *International Conference on Machine Learning (ICML)*, pages 1684–1693. PMLR, 2017.
- Yongdai Kim, Ilsang Ohn, and Dongha Kim. Fast convergence rates of deep neural networks for classification. *Neural Networks*, 138:179–197, 2021.
- Young-geun Kim, Yongchan Kwon, Hyunwoong Chang, and Myunghee Cho Paik. Lipschitz continuous autoencoders in application to anomaly detection. In *International Conference on Artificial Intelligence and Statistics (AISTATS)*, pages 2507–2517. PMLR, 2020.
- Diederik Kingma and Jimmy Ba. Adam: A method for stochastic optimization. In *International Conference on Learning Representations (ICLR)*, 2015.
- Matthew Lau, Leyan Pan, Stefan Davidov, Athanasios P Meliopoulos, and Wenke Lee. Geometric implications of classification on reducing open space risk. In *The Second Tiny Papers Track at ICLR 2024*, 2024a.
- Matthew Lau, Ismaila Seck, Athanasios P Meliopoulos, Wenke Lee, and Eugene Ndiaye. Revisiting non-separable binary classification and its applications in anomaly detection. *Transactions on Machine Learning Research*, 2024b.
- Wenke Lee and Salvatore J Stolfo. A framework for constructing features and models for intrusion detection systems. *ACM Transactions on Information and System Security (TiSSEC)*, 3(4):227–261, 2000.
- Wenke Lee and Dong Xiang. Information-theoretic measures for anomaly detection. In *Proceedings 2001 IEEE Symposium on Security and Privacy. S&P 2001*, pages 130–143, 2001.
- Wenke Lee, S.J. Stolfo, and K.W. Mok. A data mining framework for building intrusion detection models. In *Proceedings of the 1999 IEEE Symposium on Security and Privacy (Cat. No.99CB36344)*, pages 120–132, 1999.
- Zhipeng Li, Zheng Qin, Kai Huang, Xiao Yang, and Shuxiong Ye. Intrusion detection using convolutional neural networks for representation learning. In *International Conference on Neural Information Processing (NeurIPS)*, pages 858–866. Springer, 2017.
- Fei Tony Liu, Kai Ming Ting, and Zhi-Hua Zhou. Isolation forest. In *2008 Eighth IEEE International Conference on Data Mining*, pages 413–422, 2008. doi: 10.1109/ICDM.2008.17.
- Yuchen Lu and Peng Xu. Anomaly detection for skin disease images using variational autoencoder. *arXiv preprint arXiv:1807.01349*, 2018.

- Yisroel Mirsky, Tomer Doitshman, Yuval Elovici, and Asaf Shabtai. Kitsune: An ensemble of autoencoders for online network intrusion detection. In *Proceedings 2018 Network and Distributed System Security Symposium (NDSS)*. Internet Society, 2018.
- Denali Molitor, Deanna Needell, and Rachel Ward. Bias of homotopic gradient descent for the Hinge loss. *Applied Mathematics & Optimization*, 84:621–647, 2021.
- Guansong Pang, Chunhua Shen, and Anton Van Den Hengel. Deep anomaly detection with deviation networks. In *Proceedings of the 25th ACM SIGKDD international conference on knowledge discovery & data mining*, pages 353–362, 2019.
- Roberto Perdisci, Davide Ariu, Prahlad Fogla, Giorgio Giacinto, and Wenke Lee. McPAD: A multiple classifier system for accurate payload-based anomaly detection. *Computer Networks*, 53(6):864–881, 2009.
- Chen Qiu, Timo Pfommer, Marius Kloft, Stephan Mandt, and Maja Rudolph. Neural transformation learning for deep anomaly detection beyond images. In *International conference on machine learning (ICML)*, pages 8703–8714. PMLR, 2021.
- Ross Quinlan. Thyroid Disease. UCI Machine Learning Repository, 1987. DOI: <https://doi.org/10.24432/C5D010>.
- Lukas Ruff, Robert Vandermeulen, Nico Goernitz, Lucas Deecke, Shoaib Ahmed Siddiqui, Alexander Binder, Emmanuel Müller, and Marius Kloft. Deep one-class classification. In *International conference on machine learning (ICML)*, pages 4393–4402. PMLR, 2018.
- Lukas Ruff, Robert A. Vandermeulen, Nico Görnitz, Alexander Binder, Emmanuel Müller, Klaus-Robert Müller, and Marius Kloft. Deep semi-supervised anomaly detection. In *International Conference on Learning Representations (ICLR)*, 2020.
- Johannes Schmidt-Hieber. Nonparametric regression using deep neural networks with ReLU activation function. *The Annals of Statistics*, 48(4):1875–1897, 2020.
- Bernhard Schölkopf, Robert C Williamson, Alex Smola, John Shawe-Taylor, and John Platt. Support vector method for novelty detection. *Advances in neural information processing systems (NeurIPS)*, 12, 1999.
- Clayton D. Scott and Robert D. Nowak. Learning minimum volume sets. *Journal of Machine Learning Research*, 7(24):665–704, 2006.
- Tom Shenkar and Lior Wolf. Anomaly detection for tabular data with internal contrastive learning. In *International Conference on Learning Representations (ICLR)*, 2022.
- John Sipple. Interpretable, multidimensional, multimodal anomaly detection with negative sampling for detection of device failure. In *International Conference on Machine Learning (ICML)*, pages 9016–9025. PMLR, 2020.
- Ingo Steinwart, Don Hush, and Clint Scovel. A classification framework for anomaly detection. *Journal of Machine Learning Research*, 6(2), 2005.
- Taiji Suzuki. Adaptivity of deep ReLU network for learning in Besov and mixed smooth Besov spaces: optimal rate and curse of dimensionality. In *International Conference on Learning Representations (ICLR)*, 2018.

- Mahbod Tavallaee, Ebrahim Bagheri, Wei Lu, and Ali A. Ghorbani. A detailed analysis of the KDD cup 99 data set. In *2009 IEEE Symposium on Computational Intelligence for Security and Defense Applications*, pages 1–6, 2009. doi: 10.1109/CISDA.2009.5356528.
- David M.J. Tax and Robert P.W. Duin. Support vector data description. *Machine Learning*, 54(1):45–66, 2004.
- Xin Tong, Yang Feng, and Anqi Zhao. A survey on Neyman-Pearson classification and suggestions for future research. *Wiley Interdisciplinary Reviews: Computational Statistics*, 8(2):64–81, 2016.
- Alexander B Tsybakov. Optimal aggregation of classifiers in statistical learning. *The Annals of Statistics*, 32(1):135–166, 2004.
- Alexandre B Tsybakov. On nonparametric estimation of density level sets. *The Annals of Statistics*, 25(3): 948–969, 1997.
- William Henry Young. On classes of summable functions and their Fourier series. *Proceedings of the Royal Society of London. Series A, Containing Papers of a Mathematical and Physical Character*, 87(594):225–229, 1912.
- Tong Zhang. Statistical behavior and consistency of classification methods based on convex risk minimization. *The Annals of Statistics*, 32(1):56–85, 2004.
- Xianchao Zhang, Jie Mu, Xiaotong Zhang, Han Liu, Linlin Zong, and Yuangang Li. Deep anomaly detection with self-supervised learning and adversarial training. *Pattern Recognition*, 121:108234, 2022.
- Yunhe Zhang, Yan Sun, Jinyu Cai, and Jicong Fan. Deep orthogonal hypersphere compression for anomaly detection. In *The Twelfth International Conference on Learning Representations (ICLR)*, 2024.
- Panpan Zheng, Shuhan Yuan, Xintao Wu, Jun Li, and Aidong Lu. One-class adversarial nets for fraud detection. In *Proceedings of the AAAI Conference on Artificial Intelligence (AAAI)*, volume 33, pages 1286–1293, 2019.
- Tian-Yi Zhou and Xiaoming Huo. Classification of data generated by Gaussian mixture models using deep ReLU networks. *Journal of Machine Learning Research*, 25(190):1–54, 2024.
- Bo Zong, Qi Song, Martin Renqiang Min, Wei Cheng, Cristian Lumezanu, Daeki Cho, and Haifeng Chen. Deep autoencoding Gaussian mixture model for unsupervised anomaly detection. In *International Conference on Learning Representations (ICLR)*, 2018.

Appendix A Empirical Measure for Anomaly Detection/Density Level Set Estimation

In Section 2.1, we mentioned that there is limited knowledge on how to empirically estimate $S_{\mu,h,\rho}(f) := \mu(\{f > 0\} \Delta \{h > \rho\})$ with only normal samples. We proceed to give an intuition as to why it is challenging to do so. Intuitively, we use the sets $\{x \in \mathcal{X} : f(x) \leq 0\} := \{f \leq 0\}$ and $\{x \in \mathcal{X} : f(x) > 0\} := \{f > 0\}$ partition the domain \mathcal{X} into two spaces: the subspace of \mathcal{X} containing normal data and the subspace of \mathcal{X} containing anomalies. However, in unsupervised AD, we only have normal samples. So, with no knowledge of the target set $\{h > \rho\}$, many trivial solutions for the level set estimation problem may exist. Nevertheless, empirical methods can use more information to their advantage, such as how we leveraged the property of anomalies to occur less frequently than normal data.

Appendix B Auxiliary Lemma

The result from [Schmidt-Hieber, 2020] demonstrates that ReLU networks can accurately approximate any Hölder continuous function. The result is stated below. We use this result to derive an approximation error bound (see Supplement C.2) and to define our target neural network function class (i.e., hypothesis space) \mathcal{H}_τ in Definition 3.1.

Lemma 1 (Theorem 5 in [Schmidt-Hieber, 2020]). *Let $\alpha, r > 0$. For any Hölder continuous function $\eta \in \mathcal{H}^{\alpha,r}([0,1]^d)$ and for any integers $m \geq 1$ and $N \geq \max\{(\alpha+1)^d, (r+1)e^d\}$, there exists a ReLU neural network*

$$\hat{\eta} \in \mathcal{F}(L^*, w^*, v^*, K^*)$$

with depth

$$L^* = 8 + (m+5)(1 + \lceil \log_2(\max\{d, \alpha\}) \rceil),$$

maximum number of nodes

$$w^* = 6(d + \lceil \alpha \rceil)N,$$

number of nonzero parameters

$$v^* = 141(d + \alpha + 1)^{3+d}N(m+6),$$

and all parameters (absolute value) are bounded by

$$K^* = 1$$

such that

$$\|\hat{\eta} - \eta\|_{L^\infty([0,1]^d)} \leq (2r+1)(1+d^2+\alpha^2)6^d N 2^{-m} + r3^\alpha N^{-\frac{\alpha}{d}}. \quad (20)$$

Appendix C Proof of Theorem 4.1

This part presents the proof of Theorem 4.1. Specifically, we derive the convergence rate in terms of n (i.e., the size of normal training sample T) of the excess risk. We begin our analysis with a standard error decomposition (Supplement C.1) to decompose the excess generalization error $\varepsilon(\hat{f}_{T,T',\phi}) - \varepsilon(f_c)$ into two

estimation error terms and one approximation error term. After that, we estimate each of these error terms respectively (Supplement C.2 and C.3). Finally, we combine the error estimates and find the ideal parameters (Supplement C.4).

C.1 Error Decomposition

We consider the following error decomposition. Similar error decomposition can be found in [Zhou and Huo, 2024].

Lemma 2 (Decomposition of $\varepsilon(\hat{f}_{T,T',\phi}) - \varepsilon(f_c)$). *Let $f_{\mathcal{H}}$ be any function in \mathcal{H}_{τ} . There holds*

$$\varepsilon(\hat{f}_{T,T',\phi}) - \varepsilon(f_c) \leq \{\varepsilon(\hat{f}_{T,T',\phi}) - \varepsilon_{T,T'}(\hat{f}_{T,T',\phi})\} + \{\varepsilon_{T,T'}(f_{\mathcal{H}}) - \varepsilon(f_{\mathcal{H}})\} + \{\varepsilon(f_{\mathcal{H}}) - \varepsilon(f_c)\}. \quad (21)$$

Proof. We express $\varepsilon(\hat{f}_{T,T',\phi}) - \varepsilon(f_c)$ by inserting empirical risks as follows

$$\begin{aligned} \varepsilon(\hat{f}_{T,T',\phi}) - \varepsilon(f_c) &= \{\varepsilon(\hat{f}_{T,T',\phi}) - \varepsilon_{T,T'}(\hat{f}_{T,T',\phi})\} + \{\varepsilon_{T,T'}(\hat{f}_{T,T',\phi}) - \varepsilon_{T,T'}(f_{\mathcal{H}})\} \\ &+ \{\varepsilon_{T,T'}(f_{\mathcal{H}}) - \varepsilon(f_{\mathcal{H}})\} + \{\varepsilon(f_{\mathcal{H}}) - \varepsilon(f_c)\}. \end{aligned}$$

Note that both $\hat{f}_{T,T',\phi}$ and $f_{\mathcal{H}}$ lie on the hypothesis space \mathcal{H}_{τ} . From the definition of $\hat{f}_{T,T',\phi}$ at (14), $\hat{f}_{T,T',\phi}$ minimizes the empirical risk over \mathcal{H}_{τ} . Thus we have $\varepsilon_{T,T'}(\hat{f}_{T,T',\phi}) - \varepsilon_{T,T'}(f_{\mathcal{H}}) \leq 0$ for all $f_{\mathcal{H}} \in \mathcal{H}_{\tau}$. This yields the expression (21). \square

The expression $\{\varepsilon(\hat{f}_{T,T',\phi}) - \varepsilon_{T,T'}(\hat{f}_{T,T',\phi})\}$ is the first estimation error (also known as the sample error) term, $\{\varepsilon_{T,T'}(f_{\mathcal{H}}) - \varepsilon(f_{\mathcal{H}})\}$ is the second estimation error term, whereas $\{\varepsilon(f_{\mathcal{H}}) - \varepsilon(f_c)\}$ — which does not depend on the training samples — is the approximation error term induced by $f_{\mathcal{H}}$. To give an upper bound to the excess generalization error, we will proceed to bound these three error terms respectively.

We will begin with estimating the upper bound of the approximation error term $\{\varepsilon(f_{\mathcal{H}}) - \varepsilon(f_c)\}$.

C.2 Upper Bound of the Approximation Error

Note that $\sigma_{\tau}(\hat{\eta} - 1/2) \in \mathcal{H}_{\tau}$, where $\hat{\eta}$ is the approximation of the function η in Lemma 1. Recall that we use $f_{\mathcal{H}}$ to denote any functions in \mathcal{H}_{τ} . In this subsection, we derive a tight upper bound for the approximation error $\varepsilon(f_{\mathcal{H}}) - \varepsilon(f_c)$ by taking $f_{\mathcal{H}} = \sigma_{\tau}(\hat{\eta} - 1/2)$. We recall that f_c is the Bayes classifier given by $f_c = \text{sign}(\eta - 1/2)$.

Lemma 3. *Let $0 < \tau \leq 1$. Assume the Tsybakov noise condition (Assumption 2.1) holds for some noise exponent $q \in [0, \infty)$ and constant $c_0 > 0$. There holds*

$$\varepsilon(\sigma_{\tau}(\hat{\eta} - 1/2)) - \varepsilon(f_c) \leq 8c_0 (\tau + \|\hat{\eta} - \eta\|_{L^{\infty}[0,1]^d})^{q+1}. \quad (22)$$

Proof. Observe that the Hinge loss function $\phi(x) = \max\{0, 1 - x\}$ is Lipschitz continuous on \mathbb{R} because

$$|\phi(x_1) - \phi(x_2)| \leq |x_1 - x_2| \quad \forall x_1, x_2 \in \mathbb{R}. \quad (23)$$

For any f such that $|f(X)| \leq 1$, we have $\phi(Yf(X)) = 1 - Yf(X)$. Then,

$$\begin{aligned}
\varepsilon(f_{\mathcal{H}}) - \varepsilon(f_c) &= \int_{\mathcal{X}} \int_{\mathcal{Y}} 1 - Yf_{\mathcal{H}}(X) - (1 - Yf_c(X)) dP(Y|X)dP_{\mathcal{X}} \\
&= \int_{\mathcal{X}} \int_{\mathcal{Y}} -Y(f_{\mathcal{H}}(X) - f_c(X)) dP(Y|X)dP_{\mathcal{X}} \\
&= \int_{\mathcal{X}} (f_{\mathcal{H}}(X) - f_c(X)) \int_{\mathcal{Y}} -Y dP(Y|X)dP_{\mathcal{X}} \\
&\stackrel{(3)}{=} \int_{\mathcal{X}} (f_c(X) - f_{\mathcal{H}}(X))(2\eta(X) - 1) dP_{\mathcal{X}} \\
&= \int_{\mathcal{X}} |f_{\mathcal{H}}(X) - f_c(X)| |2\eta(X) - 1| dP_{\mathcal{X}}.
\end{aligned}$$

In the last equality, we have used the fact that $2\eta(X) - 1 > 0$ if and only if $f_c(X) = 1$.

Take $f_{\mathcal{H}} = \sigma_{\tau}(\widehat{\eta} - 1/2)$. We consider the cases $|\eta(X) - 1/2| \leq \epsilon$ and $|\eta(X) - 1/2| > \epsilon$ separately for $\epsilon := \|\widehat{\eta} - \eta\|_{L^{\infty}[0,1]^d}$.

Notice that

$$|f_{\mathcal{H}}(X) - f_c(X)| \leq |f_{\mathcal{H}}(X)| + |f_c(X)| \leq 2 \quad \forall X \in \mathcal{X}. \quad (24)$$

For the case $|\eta(X) - 1/2| \leq \epsilon$, it follows from the Tsybakov noise condition (Assumption 2.1) that

$$\begin{aligned}
&\int_{\{X \in \mathcal{X} : |\eta(X) - 1/2| \leq \epsilon\}} |f_{\mathcal{H}}(X) - f_c(X)| |2\eta(X) - 1| dP_{\mathcal{X}} \\
&\stackrel{(24)}{\leq} 4\epsilon \int_{\{x \in \mathcal{X} : |\eta(x) - 1/2| \leq \epsilon\}} dP_{\mathcal{X}} \\
&= 4\epsilon \cdot \mathbb{P}_{\mathcal{X}}(\{x \in \mathcal{X} : |\eta(x) - 1/2| \leq \epsilon\}) \\
&\stackrel{\text{Assumption 2.1}}{\leq} 4\epsilon \cdot c_0 \epsilon^q = 4c_0 \epsilon^{q+1}.
\end{aligned}$$

Next, for the case $|\eta(X) - 1/2| > \epsilon$, since $|\widehat{\eta}(X) - \eta(X)| \leq \epsilon$, we have $\text{sign}(\widehat{\eta}(X) - 1/2) = \text{sign}(\eta(X) - 1/2) = f_c(X)$. If $\sigma_{\tau}(\widehat{\eta}(X) - 1/2) = f_{\mathcal{H}}(X) \in \{1, -1\}$, then $f_{\mathcal{H}}(X)$ is exactly equal to $f_c(X)$, which implies

$$|\sigma_{\tau}(\widehat{\eta}(X) - 1/2) - f_c(X)| = 0. \quad (25)$$

Thus, we have

$$\begin{aligned}
&\int_{\{X \in \mathcal{X} : |\eta(X) - 1/2| > \epsilon\}} |f_{\mathcal{H}}(X) - f_c(X)| |2\eta(X) - 1| dP_{\mathcal{X}} \\
&\stackrel{(25)}{=} \int_{\{X \in \mathcal{X} : |\eta(X) - 1/2| > \epsilon, |\sigma_{\tau}(\widehat{\eta}(X) - 1/2)| < 1\}} |\sigma_{\tau}(\widehat{\eta}(X) - 1/2) - f_c(X)| |2\eta(X) - 1| dP_{\mathcal{X}} \\
&\leq 2(\tau + \epsilon) 2\mathbb{P}_{\mathcal{X}}(X \in \mathcal{X} : |\eta(X) - 1/2| > \epsilon, |\sigma_{\tau}(\widehat{\eta}(X) - 1/2)| < 1) \\
&\leq 2(\tau + \epsilon) 2\mathbb{P}_{\mathcal{X}}(X \in \mathcal{X} : |\sigma_{\tau}(\widehat{\eta}(X) - 1/2)| < 1) \\
&= 2(\tau + \epsilon) 2\mathbb{P}_{\mathcal{X}}(X \in \mathcal{X} : |\widehat{\eta}(X) - 1/2| < \tau) \\
&\leq 2(\tau + \epsilon) 2\mathbb{P}_{\mathcal{X}}(X \in \mathcal{X} : |\eta(X) - 1/2| < \tau + \epsilon) \\
&\stackrel{\text{Assumption 2.1}}{\leq} 4c_0(\tau + \epsilon)^{q+1}.
\end{aligned}$$

In the second equality, we have used the equivalence between $|\sigma_{\tau}(\widehat{\eta}(X) - 1/2)| < 1$ and $|\widehat{\eta}(X) - 1/2| < \tau$.

In the third inequality, we have used the condition $|\hat{\eta}(X) - \eta(X)| \leq \epsilon$ for getting $|\eta(X) - 1/2| < \tau + \epsilon$ when $|\hat{\eta}(X) - 1/2| < \tau$.

Combining the above estimates, we get the desired bound and prove the lemma. \square

C.3 Upper Bound of the Estimation Errors

In this subsection, we derive an upper bound of the estimation errors $\varepsilon(\hat{f}_{T,T',\phi}) - \varepsilon_{T,T'}(\hat{f}_{T,T',\phi}) + \varepsilon_{T,T'}(f_{\mathcal{H}}) - \varepsilon(f_{\mathcal{H}})$.

We first rewrite it by inserting $\varepsilon(f_c)$ and $\varepsilon_{T,T'}(f_c)$:

$$\begin{aligned} & \varepsilon(\hat{f}_{T,T',\phi}) - \varepsilon_{T,T'}(\hat{f}_{T,T',\phi}) + \varepsilon_{T,T'}(f_{\mathcal{H}}) - \varepsilon(f_{\mathcal{H}}) \\ = & \varepsilon(\hat{f}_{T,T',\phi}) - \varepsilon(f_c) - (\varepsilon_{T,T'}(\hat{f}_{T,T',\phi}) - \varepsilon_{T,T'}(f_c)) \end{aligned} \quad (26)$$

$$+ \varepsilon_{T,T'}(f_{\mathcal{H}}) - \varepsilon_{T,T'}(f_c) - (\varepsilon(f_{\mathcal{H}}) - \varepsilon(f_c)). \quad (27)$$

In other words, to bound $\varepsilon(\hat{f}_{T,T',\phi}) - \varepsilon_{T,T'}(f_z) + (\varepsilon_{T,T'}(f_{\mathcal{H}}) - \varepsilon(f_{\mathcal{H}}))$, we ought to bound the R.H.S. of (26) and the R.H.S. of (27) respectively.

C.3.1 Upper bound of the first estimation error

We will first handle the term $\varepsilon_{T,T'}(f_{\mathcal{H}}) - \varepsilon_{T,T'}(f_c) - (\varepsilon(f_{\mathcal{H}}) - \varepsilon(f_c))$, which is the R.H.S. of (27).

We define two random variables:

$$\xi(X) := \phi(f_{\mathcal{H}}(X)) - \phi(f_c(X)) \quad \text{over } (\mathcal{X}, Q) \quad (28)$$

and

$$\kappa(X) := \phi(-f_{\mathcal{H}}(X)) - \phi(-f_c(X)) \quad \text{over } (\mathcal{X}, \mu). \quad (29)$$

Then, we have

$$\begin{aligned} & \varepsilon_{T,T'}(f_{\mathcal{H}}) - \varepsilon_{T,T'}(f_c) - (\varepsilon(f_{\mathcal{H}}) - \varepsilon(f_c)) \\ = & \frac{s}{n} \sum_{i=1}^n \phi(f_{\mathcal{H}}(X_i)) + \frac{(1-s)}{n'} \sum_{i=1}^{n'} \phi(-f_{\mathcal{H}}(X'_i)) \\ & - \left(\frac{s}{n} \sum_{i=1}^n \phi(f_c(X_i)) + \frac{(1-s)}{n'} \sum_{i=1}^{n'} \phi(-f_c(X'_i)) \right) \\ & - \left[s \int_{\mathcal{X}} \phi(f_{\mathcal{H}}(X)) dQ + (1-s) \int_{\mathcal{X}} \phi(-f_{\mathcal{H}}(X)) d\mu \right. \\ & \left. - \left(s \int_{\mathcal{X}} \phi(f_c(X)) dQ + (1-s) \int_{\mathcal{X}} \phi(-f_c(X)) d\mu \right) \right] \\ \stackrel{(28),(29)}{=} & s \left(\frac{1}{n} \sum_{i=1}^n \xi(X_i) - \mathbb{E}_Q[\xi(X)] \right) + (1-s) \left(\frac{1}{n'} \sum_{i=1}^{n'} \kappa(X'_i) - \mathbb{E}_{\mu}[\kappa(X)] \right). \end{aligned} \quad (30)$$

We see that this is a function of random variables ξ and κ . We can use Bernstein's inequality to estimate $\frac{1}{n} \sum_{i=1}^n \xi(X_i) - \mathbb{E}_Q[\xi(X)]$ and $\frac{1}{n'} \sum_{i=1}^{n'} \kappa(X'_i) - \mathbb{E}_{\mu}[\kappa(X)]$ respectively. To apply Bernstein's inequality, we need first to establish upper bounds of the variance of ξ and the variance of κ .

Recall the Tsybakov noise condition we imposed in Assumption 2.1. Here, we give an upper bound of the second moment and thereby the variance of $\phi(yf(X)) - \phi(yf_c(X))$ for any function $f : \mathcal{X} \rightarrow [-1, 1]$ and some $y \in \{-1, 1\}$ with the noise condition. Note that $y \in \{-1, 1\}$ is not random here. Denote $P_{\mathcal{X}}^y = Q$ for $y = 1$, $P_{\mathcal{X}}^y = \mu$ for $y = -1$.

Lemma 4. *Let $0 \leq q \leq \infty$. If the Tsybakov noise condition holds for some noise exponent q and constant $c_0 > 0$, then for every function $f : \mathcal{X} \rightarrow [-1, 1]$ and some $y \in \{-1, 1\}$, there holds*

$$\mathbb{E}_{P_{\mathcal{X}}^y} [\{\phi(yf(X)) - \phi(yf_c(X))\}^2] \leq \frac{5}{s_y} (c_0)^{\frac{1}{q+1}} (\varepsilon(f) - \varepsilon(f_c))^{\frac{q}{q+1}}, \quad (31)$$

where

$$s_y = s \quad \text{for } y = 1 \text{ and } s_y = 1 - s \quad \text{for } y = -1. \quad (32)$$

Proof. Since $f(X) \in [-1, 1]$,

$$\phi(yf(X)) - \phi(yf_c(X)) = 1 - yf(X) - (1 - yf_c(X)) = y(f_c(X) - f(X)).$$

It follows that

$$\begin{aligned} \mathbb{E}_{P_{\mathcal{X}}^y} [\{\phi(yf(X)) - \phi(yf_c(X))\}^2] &= \mathbb{E}_{P_{\mathcal{X}}^y} [y^2(f_c(X) - f(X))^2] \\ &= \mathbb{E}_{P_{\mathcal{X}}^y} [(f_c(X) - f(X))^2] \\ &= \int_{\mathcal{X}} (f_c(X) - f(X))^2 dP_{\mathcal{X}}^y. \end{aligned}$$

Let $t > 0$. Consider these two subsets of the domain \mathcal{X} : $\mathcal{X}_t^+ = \{X \in \mathcal{X} : |\eta(X) - 1/2| > t\}$ and $\mathcal{X}_t^- = \{X \in \mathcal{X} : |\eta(X) - 1/2| \leq t\}$. On the set \mathcal{X}_t^+ , we apply $|f_c(X) - f(X)| \leq 2$ and $\frac{|\eta(X) - 1/2|}{t} > 1$ and get

$$|f_c(X) - f(X)|^2 \leq 2|f_c(X) - f(X)| \frac{|\eta(X) - 1/2|}{t} = |f_c(X) - f(X)| \frac{|2\eta(X) - 1|}{t}. \quad (33)$$

On the set \mathcal{X}_t^- , we have

$$|f_c(X) - f(X)|^2 \leq 4. \quad (34)$$

Recall from the proof of Lemma 3, we derived the expression for $\varepsilon(f) - \varepsilon(f_c)$ for any $|f(X)| \leq 1$ given by

$$\varepsilon(f) - \varepsilon(f_c) = \int_{\mathcal{X}} |f_c(X) - f(X)| |2\eta(X) - 1| dP_{\mathcal{X}}. \quad (35)$$

It follows from the Tsybakov noise condition that

$$\begin{aligned}
& \mathbb{E}_{P_{\mathcal{X}}^y} [\{\phi(yf(X)) - \phi(yf_c(X))\}^2] \\
&= \int_{\mathcal{X}} (f_c(X) - f(X))^2 dP_{\mathcal{X}}^y \\
&= \int_{\mathcal{X}_t^-} (f_c(X) - f(X))^2 dP_{\mathcal{X}}^y + \int_{\mathcal{X}_t^+} (f_c(X) - f(X))^2 dP_{\mathcal{X}}^y \\
&\stackrel{(33),(34)}{\leq} 4P_{\mathcal{X}}^y(\{x \in \mathcal{X} : |\eta(X) - 1/2| \leq t\}) + \frac{1}{t} \int_{\mathcal{X}_t^+} |f_c(X) - f(X)| |2\eta(X) - 1| dP_{\mathcal{X}}^y \\
&\stackrel{\because \mathcal{X}_t^+ \subseteq \mathcal{X}}{\leq} 4P_{\mathcal{X}}^y(\{x \in \mathcal{X} : |\eta(X) - 1/2| \leq t\}) + \frac{1}{t} \int_{\mathcal{X}} |f_c(X) - f(X)| |2\eta(X) - 1| dP_{\mathcal{X}}^y \\
&\stackrel{\text{Assumption 2.1},(32),(35)}{\leq} \frac{1}{s_y} \left\{ 4c_0 t^q + \frac{1}{t} (\varepsilon(f) - \varepsilon(f_c)) \right\}.
\end{aligned}$$

Here, in the last inequality, we have used the relations $dP_{\mathcal{X}}^y = dQ \leq \frac{1}{s} dP_{\mathcal{X}}$ for $y = 1$ and $dP_{\mathcal{X}}^y \leq \frac{1}{1-s} dP_{\mathcal{X}}$ for $y = -1$.

Now set $t = \left(\frac{\varepsilon(f) - \varepsilon(f_c)}{c_0} \right)^{1/(q+1)}$, the proof is complete. \square

The one-side Bernstein's inequality asserts for a random variable ξ on \mathcal{X} with mean μ and variance σ^2 satisfying $|\xi - \mu| \leq B$ almost surely that for a random i.i.d. sample $\{X_i\}_{i=1}^n$ and every $t > 0$,

$$\text{Prob} \left\{ \mu - \frac{1}{n} \sum_{i=1}^n \xi(X_i) > t \right\} \leq \exp \left\{ -\frac{nt^2}{2(\sigma^2 + \frac{1}{3}Bt)} \right\}. \quad (36)$$

We now apply Bernstein's inequality to obtain a high probability upper bound of $\varepsilon_{T,T'}(f_{\mathcal{H}}) - \varepsilon_{T,T'}(f_c) - (\varepsilon(f_{\mathcal{H}}) - \varepsilon(f_c))$.

Lemma 5. *Suppose the noise condition (Assumption 2.1) holds for some $q \in [0, \infty]$ and constant $c_0 > 0$. For any $0 < \delta < 1$, with probability $1 - \frac{\delta}{2}$, we have*

$$\begin{aligned}
& \varepsilon_{T,T'}(f_{\mathcal{H}}) - \varepsilon_{T,T'}(f_c) - (\varepsilon(f_{\mathcal{H}}) - \varepsilon(f_c)) \\
&\leq C_q \left(\log \left(\frac{4}{\delta} \right) \right) \left(s^{\frac{1}{q+2}} \left(\frac{1}{n} \right)^{\frac{q+1}{q+2}} + (1-s)^{\frac{1}{q+2}} \left(\frac{1}{n'} \right)^{\frac{q+1}{q+2}} \right) + \frac{(\varepsilon(f_{\mathcal{H}}) - \varepsilon(f_c))}{2}, \quad (37)
\end{aligned}$$

where C_q is a positive constant depending only on q and c_0 .

Proof. Recall that from Lemma 4, we know for every function $f : \mathcal{X} \rightarrow [-1, 1]$ and some $y \in \{-1, 1\}$,

$$\mathbb{E}_{P_{\mathcal{X}}^y} [\{\phi(yf(X)) - \phi(yf_c(X))\}^2] \leq \frac{5}{s_y} (c_0)^{\frac{1}{q+1}} (\varepsilon(f) - \varepsilon(f_c))^{\frac{q}{q+1}}.$$

Then the variance σ^2 of the random variable ξ for $y = 1$ and κ for $y = -1$ is bounded by

$$\sigma^2 \leq \frac{5}{s_y} (c_0)^{\frac{1}{q+1}} (\varepsilon(f_{\mathcal{H}}) - \varepsilon(f_c))^{\frac{q}{q+1}}, \quad (38)$$

where $s_y = s$ for $y = 1$ and $s_y = 1 - s$ for $y = -1$.

By the one-sided Bernstein's inequality (36), for any $\epsilon > 0$, there holds, with probability at least $1 -$

$$\exp\left(-\frac{n\epsilon^2}{2(\sigma^2+2\epsilon/3)}\right),$$

$$\left(\frac{1}{n}\sum_{i=1}^n \xi(X_i) - \mathbb{E}_Q[\xi(X)]\right) \leq \epsilon.$$

Setting this confidence bound to be $1 - \frac{\delta}{4}$, we obtain a quadratic equation for ϵ as follow

$$\log\left(\frac{4}{\delta}\right) = \frac{n\epsilon^2}{2(\sigma^2 + 2\epsilon/3)}.$$

We solve this equation and get a positive solution ϵ^* given by

$$\begin{aligned} \epsilon^* &= \frac{\frac{4}{3}\log\left(\frac{4}{\delta}\right) + \sqrt{\frac{16}{9}\log^2\left(\frac{4}{\delta}\right) + 8n\sigma^2\log\left(\frac{4}{\delta}\right)}}{2n} \\ &\leq \frac{2}{3n}\log\left(\frac{4}{\delta}\right) + \frac{2}{3n}\log\left(\frac{4}{\delta}\right) + \frac{\sqrt{2\sigma^2\log\left(\frac{4}{\delta}\right)}}{\sqrt{n}} \\ &\stackrel{(38)}{\leq} \frac{4}{3n}\log\left(\frac{4}{\delta}\right) + 4\frac{\sqrt{\log\left(\frac{4}{\delta}\right)}}{\sqrt{ns}}(c_0)^{\frac{1}{2(q+1)}}(\varepsilon(f_{\mathcal{H}}) - \varepsilon(f_c))^{\frac{q}{2(q+1)}}. \end{aligned}$$

Consider the classic Young's Inequality for products [Young, 1912] given by

$$a \cdot b \leq \frac{a^p}{p} + \frac{b^{p^*}}{p^*} \quad \text{with } a \geq 0, b \geq 0, p > 1, p^* > 1 \text{ and } \frac{1}{p} + \frac{1}{p^*} = 1. \quad (39)$$

Applying Young's Inequality with $a = 4\frac{\sqrt{\log\left(\frac{4}{\delta}\right)}}{\sqrt{ns}}(c_0)^{\frac{1}{2(q+1)}}$, $b = (\varepsilon(f_{\mathcal{H}}) - \varepsilon(f_c))^{\frac{q}{2(q+1)}}$, $p = \frac{2(q+1)}{q+2}$, $p^* = \frac{2(q+1)}{q}$, we got

$$\begin{aligned} \epsilon^* &\leq \frac{4}{3n}\log\left(\frac{4}{\delta}\right) + 4\frac{\sqrt{\log\left(\frac{4}{\delta}\right)}}{\sqrt{ns}}(c_0)^{\frac{1}{2(q+1)}}(\varepsilon(f_{\mathcal{H}}) - \varepsilon(f_c))^{\frac{q}{2(q+1)}} \\ &\leq \frac{4}{3n}\log\left(\frac{4}{\delta}\right) + \left(\frac{q+2}{2(q+1)}\right)\left(4\frac{\sqrt{\log\left(\frac{4}{\delta}\right)}}{\sqrt{ns}}(c_0)^{\frac{1}{2(q+1)}}\right)^{\frac{2(q+1)}{q+2}} + \frac{\varepsilon(f_{\mathcal{H}}) - \varepsilon(f_c)}{\frac{2(q+1)}{q}}. \end{aligned} \quad (40)$$

Similarly, we use the same approach to obtain that, with a probability of at least $1 - \frac{\delta}{4}$,

$$\begin{aligned} &\left(\frac{1}{n'}\sum_{i=1}^{n'} \kappa(X'_i) - \mathbb{E}_\mu[\kappa(X')]\right) \\ &\leq \frac{4}{3n'}\log\left(\frac{4}{\delta}\right) + \left(\frac{q+2}{2(q+1)}\right)\left(4\frac{\sqrt{\log\left(\frac{4}{\delta}\right)}}{\sqrt{n'(1-s)}}(c_0)^{\frac{1}{2(q+1)}}\right)^{\frac{2(q+1)}{q+2}} + \frac{\varepsilon(f_{\mathcal{H}}) - \varepsilon(f_c)}{\frac{2(q+1)}{q}}. \end{aligned} \quad (41)$$

Now, combining the above error bounds, we get, with probability of at least $1 - \frac{\delta}{2}$,

$$\begin{aligned}
& \varepsilon_{T, T'}(f_{\mathcal{H}}) - \varepsilon_{T, T'}(f_c) - (\varepsilon(f_{\mathcal{H}}) - \varepsilon(f_c)) \\
\stackrel{(30)}{=} & s \left(\frac{1}{n} \sum_{i=1}^n \xi(X_i) - \mathbb{E}[\xi(X)] \right) + (1-s) \left(\frac{1}{n'} \sum_{i=1}^{n'} \kappa(X'_i) - \mathbb{E}[\kappa(X')] \right) \\
\stackrel{(40), (41)}{\leq} & s \left(\frac{4}{3n} \log \left(\frac{4}{\delta} \right) + \left(\frac{q+2}{2(q+1)} \right) \left(4 \frac{\sqrt{\log \left(\frac{4}{\delta} \right)}}{\sqrt{ns}} (c_0)^{\frac{1}{2(q+1)}} \right)^{\frac{2(q+1)}{q+2}} + \frac{\varepsilon(f_{\mathcal{H}}) - \varepsilon(f_c)}{\frac{2(q+1)}{q}} \right) \\
& + (1-s) \left[\frac{4}{3n'} \log \left(\frac{4}{\delta} \right) + \left(\frac{q+2}{2(q+1)} \right) \left(4 \frac{\sqrt{\log \left(\frac{4}{\delta} \right)}}{\sqrt{n'(1-s)}} (c_0)^{\frac{1}{2(q+1)}} \right)^{\frac{2(q+1)}{q+2}} \right. \\
& \quad \left. + \frac{\varepsilon(f_{\mathcal{H}}) - \varepsilon(f_c)}{\frac{2(q+1)}{q}} \right] \\
\leq & \frac{4}{3} \left(\frac{s}{n} + \frac{1-s}{n'} \right) \log \left(\frac{4}{\delta} \right) \\
& + 4^{\frac{2(q+1)}{q+2}} (c_0)^{\frac{q}{2(q+1)}} \left(\log \left(\frac{4}{\delta} \right) \right)^{\frac{q+1}{q+2}} \left(s^{\frac{1}{q+2}} \left(\frac{1}{n} \right)^{\frac{q+1}{q+2}} + (1-s)^{\frac{1}{q+2}} \left(\frac{1}{n'} \right)^{\frac{q+1}{q+2}} \right) \\
& + \left(\frac{q}{2(q+1)} \right) (\varepsilon(f_{\mathcal{H}}) - \varepsilon(f_c)) \\
\leq & C_q \left(\log \left(\frac{4}{\delta} \right) \right) \left(s^{\frac{1}{q+2}} \left(\frac{1}{n} \right)^{\frac{q+1}{q+2}} + (1-s)^{\frac{1}{q+2}} \left(\frac{1}{n'} \right)^{\frac{q+1}{q+2}} \right) + \frac{(\varepsilon(f_{\mathcal{H}}) - \varepsilon(f_c))}{2},
\end{aligned}$$

where C_q is a positive constant depending only on q and c_0 . In the last inequality, we have used the facts that $s \leq s^{\frac{1}{q+2}}$, $1-s \leq (1-s)^{\frac{1}{q+2}}$ for all $s \in (0, 1]$ and $q > 0$; and that $\frac{1}{n} \leq \left(\frac{1}{n}\right)^{\frac{q+1}{q+2}}$, $\frac{1}{n'} \leq \left(\frac{1}{n'}\right)^{\frac{q+1}{q+2}}$. The proof is complete. \square

C.3.2 Upper bound of the second estimation error

Next, we will handle estimate the term $\varepsilon(\hat{f}_{T, T', \phi}) - \varepsilon(f_c) - (\varepsilon_{T, T'}(\hat{f}_{T, T', \phi}) - \varepsilon_{T, T'}(f_c))$, which is the R.H.S. of (26). We will derive an upper bound for this error term using a concentration inequality in terms of covering numbers.

For $\epsilon > 0$, denote by $\mathcal{N}(\epsilon, \mathcal{H}) := \mathcal{N}(\epsilon, \mathcal{H}, \|\cdot\|_{\infty})$ the ϵ -covering number of a set of functions \mathcal{H} with respect to $\|\cdot\|_{\infty} := \text{ess sup}_{x \in \mathcal{X}} |f(x)|$. More specifically, $\mathcal{N}(\epsilon, \mathcal{H})$ is the minimal $M \in \mathbb{N}$ such that there exists functions $\{f_1, \dots, f_M\} \in \mathcal{H}$ satisfying

$$\min_{1 \leq i \leq M} \|f - f_i\|_{\infty} \leq \epsilon, \quad \forall f \in \mathcal{H}. \tag{42}$$

The following Proposition gives an upper bound of the ϵ -covering number of a function set generated by neural networks.

Proposition 1 (Lemma 3 of [Suzuki, 2018], Lemma 5 of [Schmidt-Hieber, 2020]). *For any $\epsilon > 0$, we have*

$$\log \mathcal{N}(\epsilon, \mathcal{F}(L, w, s, K)) \leq 2L(s+1) \log(\epsilon^{-1}(L+1)(w+1)(\max\{K, 1\})). \tag{43}$$

We apply the above Proposition to obtain an estimate of the ϵ -covering number of our hypothesis space \mathcal{H}_τ .

Corollary 1 (ϵ -covering number of hypothesis space \mathcal{H}_τ). *Recall the hypothesis space defined in Definition 1 for some $0 < \tau \leq 1$*

$$\mathcal{H}_\tau := \text{span}\{\sigma_\tau(f(X)) : f \in \mathcal{F}(L^*, w^*, s^*, K^*)\}$$

with $\alpha, r > 0$, integers $m \geq 1$ and $N \geq \max\{(\alpha + 1)^d, (r + 1)e^d\}$, $L^* = 8 + (m + 5)(1 + \lceil \log_2(\max\{d, \alpha\}) \rceil)$, $w^* = 6(d + \lceil \alpha \rceil)N$, $s^* = 141(d + \alpha + 1)^{3+d}N(m + 6)$, and $K^* = 1$.

For any $0 < \epsilon \leq 1$, we have

$$\log \mathcal{N}(\epsilon, \mathcal{H}_\tau) \leq c_{\alpha, d} m^2 N \log((\tau \epsilon)^{-1} m N), \quad (44)$$

where $c_{\alpha, d}$ is a positive constant independent of r, m, N, τ or ϵ .

Proof. It follows from Proposition 1 that

$$\begin{aligned} & \log \mathcal{N}(\epsilon, \mathcal{F}(L^*, w^*, s^*, K^*)) \\ & \stackrel{(43)}{\leq} 2L^*(s^* + 1) \log(\epsilon^{-1}(L^* + 1)(w^* + 1)(\max\{K^*, 1\})) \\ & \leq 2(8 + (m + 5)(1 + \lceil \log_2(\max\{d, \alpha\}) \rceil))(141(d + \alpha + 1)^{3+d}N(m + 6) + 1) \\ & \quad \log(\epsilon^{-1}(8 + (m + 5)(1 + \lceil \log_2(\max\{d, \alpha\}) \rceil) + 1)(6(d + \lceil \alpha \rceil)N + 1)) \\ & \leq c_{\alpha, d} m^2 N \log(\epsilon^{-1} m N), \end{aligned}$$

where $c_{\alpha, d}$ is a positive constant independent of r, m, N, τ or ϵ .

Recall the function σ_τ defined in (12) for $0 < \tau \leq 1$. We observe that

$$|\sigma_\tau(u) - \sigma_\tau(v)| \leq \frac{1}{\tau} |u - v|, \quad \forall u, v \in \mathbb{R}. \quad (45)$$

It follows that for all $f, f' \in \mathcal{F}(L^*, w^*, s^*, K^*)$, $X \in \mathcal{X}$,

$$|\sigma_\tau(f(X)) - \sigma_\tau(f'(X))| \leq \frac{1}{\tau} |f(X) - f'(X)| \leq \frac{1}{\tau} \|f - f'\|_\infty.$$

Thus, we have

$$\log \mathcal{N}(\epsilon, \mathcal{H}_\tau) \leq \log \mathcal{N}(\tau \epsilon, \mathcal{F}(L^*, w^*, s^*, K^*)) = c_{\alpha, d} m^2 N \log((\tau \epsilon)^{-1} m N).$$

□

Next, by applying the one-side Bernstein's Inequality (given in (36)), we have the following result for a fixed function $f : \mathcal{X} \rightarrow [-1, 1]$.

Lemma 6. *Suppose the Tsybakov noise condition (Assumption 2.1) holds for some $q \in [0, \infty]$ and $c_0 > 0$. Let $f : \mathcal{X} \rightarrow [-1, 1]$. Then for every $\epsilon > 0$, there holds*

$$\frac{\varepsilon(f) - \varepsilon(f_c) - (\varepsilon_{T, T'}(f) - \varepsilon_{T, T'}(f_c))}{\left((\varepsilon(f) - \varepsilon(f_c))^{\frac{q}{q+1}} + \epsilon^{\frac{q}{q+1}} \right)^{1/2}} \leq 2\epsilon^{1 - \frac{q}{2(q+1)}}$$

with probability at least

$$1 - \exp \left\{ - \frac{n\epsilon^{2-\frac{q}{q+1}}}{s \left(10(c_0)^{\frac{1}{q+1}} + 2\epsilon^{1-\frac{q}{q+1}} \right)} \right\} - \exp \left\{ - \frac{n'\epsilon^{2-\frac{q}{q+1}}}{(1-s) \left(10(c_0)^{\frac{1}{q+1}} + 2\epsilon^{1-\frac{q}{q+1}} \right)} \right\}.$$

Proof. Consider the random variable $\xi(X) = s(\phi(f(X)) - \phi(f_c(X)))$ on (\mathcal{X}, Q) with $f : \mathcal{X} \rightarrow [-1, 1]$ and $s \in (0, 1)$. It satisfies $|\xi| \leq 2s$ and thereby $|\xi - \mathbb{E}[\xi]| \leq 4s$ almost surely. Moreover, by Lemma 4, when the noise condition is satisfied, we have $\sigma^2 := \text{Var}[\xi] \leq 5s(c_0)^{\frac{1}{q+1}} (\varepsilon(f) - \varepsilon(f_c))^{\frac{q}{q+1}}$. Applying the one-side Bernstein inequality (36) to this random variable and $t = \left((\varepsilon(f) - \varepsilon(f_c))^{\frac{q}{q+1}} + \epsilon^{\frac{q}{q+1}} \right)^{1/2} \epsilon^{1-\frac{q}{2(q+1)}}$ with $\epsilon > 0$, we know that

$$\begin{aligned} & s \left(\int_{\mathcal{X}} (\phi(f(X)) - \phi(f_c(X))) dQ - \frac{1}{n} \sum_{i=1}^n (\phi(f(X_i)) - \phi(f_c(X_i))) \right) \\ & \leq \left((\varepsilon(f) - \varepsilon(f_c))^{\frac{q}{q+1}} + \epsilon^{\frac{q}{q+1}} \right)^{1/2} \epsilon^{1-\frac{q}{2(q+1)}} \end{aligned}$$

with a probability of at least

$$\begin{aligned} & 1 - \exp \left\{ - \frac{n \left((\varepsilon(f) - \varepsilon(f_c))^{\frac{q}{q+1}} + \epsilon^{\frac{q}{q+1}} \right) \epsilon^{2-\frac{q}{q+1}}}{2 \left(5s(c_0)^{\frac{1}{q+1}} (\varepsilon(f) - \varepsilon(f_c))^{\frac{q}{q+1}} + \frac{4s}{3} \left((\varepsilon(f) - \varepsilon(f_c))^{\frac{q}{q+1}} + \epsilon^{\frac{q}{q+1}} \right)^{1/2} \epsilon^{1-\frac{q}{2(q+1)}} \right)} \right\} \\ & \geq 1 - \exp \left\{ - \frac{n\epsilon^{2-\frac{q}{q+1}}}{s \left(10(c_0)^{\frac{1}{q+1}} + 2\epsilon^{1-\frac{q}{q+1}} \right)} \right\}. \end{aligned}$$

In the same way, applying the one-side Bernstein inequality to the random variable $(1-s)(\phi(-f(X)) - \phi(-f_c(X)))$ on (\mathcal{X}, μ) , we find that

$$\begin{aligned} & (1-s) \left(\int_{\mathcal{X}} (\phi(-f(X)) - \phi(-f_c(X))) d\mu - \frac{1}{n'} \sum_{i=1}^{n'} (\phi(-f(X'_i)) - \phi(-f_c(X'_i))) \right) \\ & \leq \left((\varepsilon(f) - \varepsilon(f_c))^{\frac{q}{q+1}} + \epsilon^{\frac{q}{q+1}} \right)^{1/2} \epsilon^{1-\frac{q}{2(q+1)}} \end{aligned}$$

with probability at least

$$1 - \exp \left\{ - \frac{n'\epsilon^{2-\frac{q}{q+1}}}{(1-s) \left(10(c_0)^{\frac{1}{q+1}} + 2\epsilon^{1-\frac{q}{q+1}} \right)} \right\}.$$

Combining the above two estimates proves the desired inequality. \square

Lemma 7. *Let \mathcal{H} be a set of measurable functions from \mathcal{X} to $[-1, 1]$. Suppose the noise condition (Assumption 1) holds for some $q \in [0, \infty]$ and $c_0 > 0$. Then for every $\epsilon > 0$,*

$$\sup_{f \in \mathcal{H}} \frac{\varepsilon(f) - \varepsilon(f_c) - (\varepsilon_{T, T'}(f) - \varepsilon_{T, T'}(f_c))}{\left((\varepsilon(f) - \varepsilon(f_c))^{\frac{q}{q+1}} + \epsilon^{\frac{q}{q+1}} \right)^{1/2}} \leq 5\epsilon^{1-\frac{q}{2(q+1)}}$$

with probability at least

$$1 - \mathcal{N}(\epsilon, \mathcal{H}) \left\{ \exp \left\{ -\frac{n\epsilon^{2-\frac{q}{q+1}}}{s \left(10(c_0)^{\frac{1}{q+1}} + 2\epsilon^{1-\frac{q}{q+1}} \right)} \right\} + \exp \left\{ -\frac{n'\epsilon^{2-\frac{q}{q+1}}}{(1-s) \left(10(c_0)^{\frac{1}{q+1}} + 2\epsilon^{1-\frac{q}{q+1}} \right)} \right\} \right\}.$$

Proof. Let $\{f_j\}_{j=1}^{\mathcal{N}}$ be an ϵ -net of \mathcal{H} with $\mathcal{N} := \mathcal{N}(\epsilon, \mathcal{H})$. Then for each $f \in \mathcal{H}$ there exists some $j \in \{1, \dots, \mathcal{N}\}$ such that $\|f - f_j\|_\infty \leq \epsilon$. It follows that $\|\phi(f(X)) - \phi(f_j(X))\|_\infty \leq \epsilon$ and then

$$|\varepsilon(f) - \varepsilon(f_j)| \leq s\epsilon + (1-s)\epsilon = \epsilon \quad (46)$$

and

$$|\varepsilon_{T,T'}(f) - \varepsilon_{T,T'}(f_j)| \leq \epsilon. \quad (47)$$

It also implies

$$(\varepsilon(f_j) - \varepsilon(f_c))^{\frac{q}{q+1}} + \epsilon^{\frac{q}{q+1}} \stackrel{(46)}{\leq} (\varepsilon(f) - \varepsilon(f_c))^{\frac{q}{q+1}} + \epsilon^{\frac{q}{q+1}} + \epsilon^{\frac{q}{q+1}} \leq 2 \left((\varepsilon(f) - \varepsilon(f_c))^{\frac{q}{q+1}} + \epsilon^{\frac{q}{q+1}} \right)$$

and thereby

$$\begin{aligned} & \frac{\varepsilon(f) - \varepsilon(f_c) - (\varepsilon_{T,T'}(f) - \varepsilon_{T,T'}(f_c))}{\left((\varepsilon(f) - \varepsilon(f_c))^{\frac{q}{q+1}} + \epsilon^{\frac{q}{q+1}} \right)^{1/2}} \\ & \stackrel{(46),(47)}{\leq} \frac{\varepsilon(f_j) - \varepsilon(f_c) - (\varepsilon_{T,T'}(f_j) - \varepsilon_{T,T'}(f_c)) + 2\epsilon}{\left((\varepsilon(f) - \varepsilon(f_c))^{\frac{q}{q+1}} + \epsilon^{\frac{q}{q+1}} \right)^{1/2}} \\ & \leq \frac{\varepsilon(f_j) - \varepsilon(f_c) - (\varepsilon_{T,T'}(f_j) - \varepsilon_{T,T'}(f_c))}{\left(\frac{1}{2} \left((\varepsilon(f_j) - \varepsilon(f_c))^{\frac{q}{q+1}} + \epsilon^{\frac{q}{q+1}} \right) \right)^{1/2}} + 2\epsilon^{1-\frac{q}{2(q+1)}}. \end{aligned}$$

This tells us that

$$\frac{\varepsilon(f) - \varepsilon(f_c) - (\varepsilon_{T,T'}(f) - \varepsilon_{T,T'}(f_c))}{\left((\varepsilon(f) - \varepsilon(f_c))^{\frac{q}{q+1}} + \epsilon^{\frac{q}{q+1}} \right)^{1/2}} > 5\epsilon^{1-\frac{q}{2(q+1)}}$$

implies

$$\frac{\varepsilon(f_j) - \varepsilon(f_c) - (\varepsilon_{T,T'}(f_j) - \varepsilon_{T,T'}(f_c))}{\left((\varepsilon(f_j) - \varepsilon(f_c))^{\frac{q}{q+1}} + \epsilon^{\frac{q}{q+1}} \right)^{1/2}} > 2\epsilon^{1-\frac{q}{2(q+1)}}.$$

Therefore, the event

$$\sup_{f \in \mathcal{H}} \frac{\varepsilon(f) - \varepsilon(f_c) - (\varepsilon_{T,T'}(f) - \varepsilon_{T,T'}(f_c))}{\left((\varepsilon(f) - \varepsilon(f_c))^{\frac{q}{q+1}} + \epsilon^{\frac{q}{q+1}} \right)^{1/2}} > 5\epsilon^{1-\frac{q}{2(q+1)}}$$

is contained in the event

$$\bigcup_{j=1}^{\mathcal{N}} \left\{ \frac{\varepsilon(f_j) - \varepsilon(f_c) - (\varepsilon_{T,T'}(f_j) - \varepsilon_{T,T'}(f_c))}{\left((\varepsilon(f_j) - \varepsilon(f_c))^{\frac{q}{q+1}} + \epsilon^{\frac{q}{q+1}} \right)^{1/2}} > 2\epsilon^{1-\frac{q}{2(q+1)}} \right\}.$$

Then, our conclusion follows from Lemma 6. □

We shall next apply the covering number estimate of the hypothesis space \mathcal{H}_τ (given in Corollary 1) and Lemma 7 to derive a high probability upper bound of the estimation error term $\varepsilon(f) - \varepsilon(f_c) - (\varepsilon_{T,T'}(f) - \varepsilon_{T,T'}(f_c))$, which is the R.H.S. of (26).

Lemma 8. *Let $0 \leq q \leq \infty$. Let $\alpha, r > 0$, and integers $m \geq 1$ and $N \geq \max\{(\alpha + 1)^d, (r + 1)e^d\}$. Suppose the noise condition (Assumption 2.1) holds for some q and constant $c_0 > 0$. Suppose $\tau \geq \max\{\frac{1}{n}, \frac{1}{n'}\}$. For any $0 < \delta < 1$ and $n \geq 3$, with probability $1 - \frac{\delta}{2}$, we have*

$$\begin{aligned} & \varepsilon(\hat{f}_{T,T',\phi}) - \varepsilon(f_c) - (\varepsilon_{T,T'}(f) - \varepsilon_{T,T'}(f_c)) \\ & \leq C_{q,\alpha,d} \left(\log\left(\frac{4}{\delta}\right) + m^2 N (\log(nmN) + \log(n'mN)) \right)^{\frac{q+2}{q+1}} \\ & \quad \cdot \left(\max\left\{ \frac{s}{n} \log\left(\frac{n}{s}\right), \frac{(1-s)}{n'} \log\left(\frac{n'}{1-s}\right) \right\} \right)^{\frac{q+2}{q+1}} + \frac{\varepsilon(\hat{f}_{T,T',\phi}) - \varepsilon(f_c)}{2}, \end{aligned}$$

where $C_{q,\alpha,d}$ is a positive constant depending only on q, c_0, α , and d . Additionally, if $n' \in \mathbb{N}$ satisfies $(\frac{1-s}{s})n \leq n' \leq n$, with probability $1 - \frac{\delta}{2}$, we have

$$\begin{aligned} & \varepsilon(\hat{f}_{T,T',\phi}) - \varepsilon(f_c) - (\varepsilon_{T,T'}(f) - \varepsilon_{T,T'}(f_c)) \\ & \leq C_{q,\alpha,d} \left(\log\left(\frac{4}{\delta}\right) + 2m^2 N \log(nmN) \right)^{\frac{q+2}{q+1}} \left(\frac{s}{n} \log\left(\frac{n}{s}\right) \right)^{\frac{q+2}{q+1}} + \frac{\varepsilon(\hat{f}_{T,T',\phi}) - \varepsilon(f_c)}{2}. \quad (48) \end{aligned}$$

Proof. Lemma 7 tells us that, for every $0 < \epsilon \leq 1$, with probability at least

$$\begin{aligned} & 1 - \mathcal{N}(\epsilon, \mathcal{H}_\tau) \left\{ \exp\left\{ -\frac{n\epsilon^{2-\frac{q}{q+1}}}{s \left(10(c_0)^{\frac{1}{q+1}} + 2\epsilon^{1-\frac{q}{q+1}}\right)} \right\} + \exp\left\{ -\frac{n'\epsilon^{2-\frac{q}{q+1}}}{(1-s) \left(10(c_0)^{\frac{1}{q+1}} + 2\epsilon^{1-\frac{q}{q+1}}\right)} \right\} \right\} \\ & \geq 1 - \mathcal{N}(\epsilon, \mathcal{H}_\tau) \left\{ \exp\left\{ -\frac{n\epsilon^{2-\frac{q}{q+1}}}{s \left(10(c_0)^{\frac{1}{q+1}} + 2\right)} \right\} + \exp\left\{ -\frac{n'\epsilon^{2-\frac{q}{q+1}}}{(1-s) \left(10(c_0)^{\frac{1}{q+1}} + 2\right)} \right\} \right\} \\ & \stackrel{(44)}{\geq} 1 - \exp\left\{ c_{\alpha,d} m^2 N \log((\tau\epsilon)^{-1} mN) - \frac{n\epsilon^{2-\frac{q}{q+1}}}{s \left(10(c_0)^{\frac{1}{q+1}} + 2\right)} \right\} \\ & \quad - \exp\left\{ c_{\alpha,d} m^2 N \log((\tau\epsilon)^{-1} mN) - \frac{n'\epsilon^{2-\frac{q}{q+1}}}{(1-s) \left(10(c_0)^{\frac{1}{q+1}} + 2\right)} \right\}, \end{aligned}$$

there holds

$$\sup_{f \in \mathcal{H}} \frac{\varepsilon(f) - \varepsilon(f_c) - (\varepsilon_{T,T'}(f) - \varepsilon_{T,T'}(f_c))}{\left((\varepsilon(f) - \varepsilon(f_c))^{\frac{q}{q+1}} + \epsilon^{\frac{q}{q+1}} \right)^{1/2}} \leq 5\epsilon^{1-\frac{q}{2(q+1)}},$$

which implies

$$\varepsilon(f) - \varepsilon(f_c) - (\varepsilon_{T,T'}(f) - \varepsilon_{T,T'}(f_c)) \leq 5\epsilon^{1-\frac{q}{2(q+1)}} \left((\varepsilon(f) - \varepsilon(f_c))^{\frac{q}{q+1}} + \epsilon^{\frac{q}{q+1}} \right)^{1/2}, \quad \forall f \in \mathcal{H}_\tau. \quad (49)$$

We choose τ satisfying $\tau \geq \max\{\frac{1}{n}, \frac{1}{n'}\}$. Then we know $\tau^{-1} \leq n$ and $\tau^{-1} \leq n'$. We set the above

confidence bound to be at least $1 - \delta/2$. We need to find ϵ that satisfies the following two inequalities:

$$\exp \left\{ c_{\alpha,d} m^2 N \log(\epsilon^{-1} n m N) - \frac{n \epsilon^{2 - \frac{q}{q+1}}}{s \left(10(c_0)^{\frac{1}{q+1}} + 2 \right)} \right\} \leq \frac{\delta}{4}$$

and

$$\exp \left\{ c_{\alpha,d} m^2 N \log(\epsilon^{-1} n' m N) - \frac{n' \epsilon^{2 - \frac{q}{q+1}}}{(1-s) \left(10(c_0)^{\frac{1}{q+1}} + 2 \right)} \right\} \leq \frac{\delta}{4}.$$

Let $\hat{\epsilon} = \epsilon^{2 - \frac{q}{q+1}}$ and let $c_q = 10(c_0)^{\frac{1}{q+1}} + 2$. We see that c_q is a positive constant depending only on q and c_0 . We need to find $\hat{\epsilon} > 0$ such that

$$\frac{c_{\alpha,d}}{2 - \frac{q}{q+1}} m^2 N \log(\hat{\epsilon}^{-1}) - \frac{n \hat{\epsilon}}{s c_q} \leq \log \left(\frac{\delta}{4} \right) - c_{\alpha,d} m^2 N \log(n m N) \quad (50)$$

and

$$\frac{c_{\alpha,d}}{2 - \frac{q}{q+1}} m^2 N \log(\hat{\epsilon}^{-1}) - \frac{n' \hat{\epsilon}}{(1-s) c_q} \leq \log \left(\frac{\delta}{4} \right) - c_{\alpha,d} m^2 N \log(n' m N). \quad (51)$$

We define a function $T : (0, \infty) \rightarrow \mathbb{R}$ given by

$$T(x) = \frac{c_{\alpha,d}}{2 - \frac{q}{q+1}} m^2 N \log(x^{-1}) - \frac{n x}{s c_q}. \quad (52)$$

We notice that T is a decreasing function. Then, we take

$$B := c_q \left(\frac{2 c_{\alpha,d}}{2 - \frac{q}{q+1}} m^2 N + \log \left(\frac{4}{\delta} \right) + c_{\alpha,d} m^2 N \log(n m N) \right). \quad (53)$$

For $n \geq 3$ (i.e., $\log(n) > 1$), there holds

$$\frac{B s \log \left(\frac{n}{s} \right)}{n} \geq \frac{s}{n}. \quad (54)$$

It follows that

$$\begin{aligned} & T \left(\frac{B s \log \left(\frac{n}{s} \right)}{n} \right) \\ \stackrel{(52)}{=} & \frac{c_{\alpha,d}}{2 - \frac{q}{q+1}} m^2 N \log \left(\frac{n}{B s \log \left(\frac{n}{s} \right)} \right) - \frac{n}{s c_q} \left(\frac{B s \log \left(\frac{n}{s} \right)}{n} \right) \\ \stackrel{(53), (54)}{\leq} & \frac{c_{\alpha,d}}{2 - \frac{q}{q+1}} m^2 N \log \left(\frac{n}{s} \right) \\ & - \log \left(\frac{n}{s} \right) \left(\frac{c_{\alpha,d}}{2 - \frac{q}{q+1}} m^2 N + \log \left(\frac{4}{\delta} \right) + c_{\alpha,d} m^2 N \log(n m N) \right) \\ = & - \log \left(\frac{n}{s} \right) \left(\log \left(\frac{4}{\delta} \right) + c_{\alpha,d} m^2 N \log(n m N) \right) \\ \stackrel{\because \log \left(\frac{n}{s} \right) > 1}{\leq} & \log \left(\frac{\delta}{4} \right) - c_{\alpha,d} m^2 N \log(n m N). \end{aligned}$$

Since T is a decreasing function, we know that if

$$\hat{\epsilon} \geq \frac{Bs \log\left(\frac{n}{s}\right)}{n},$$

then such a $\hat{\epsilon}$ satisfies the first inequality (50). In the same way, we know that if

$$\hat{\epsilon} \geq \frac{B'(1-s)}{n'} \log\left(\frac{n'}{1-s}\right)$$

with

$$B' := c_q \left(\frac{2c_{\alpha,d}}{2 - \frac{q}{q+1}} m^2 N + \log\left(\frac{4}{\delta}\right) + c_{\alpha,d} m^2 N \log(n' m N) \right),$$

then such a $\hat{\epsilon}$ satisfies the second inequality (51).

We choose $\hat{\epsilon}$ to be

$$\hat{\epsilon} = \max \left\{ \frac{Bs \log\left(\frac{n}{s}\right)}{n}, \frac{B'(1-s)}{n'} \log\left(\frac{n'}{1-s}\right) \right\}.$$

Thus, $\hat{\epsilon}$ satisfies both inequalities (50) and (51). Then, we have

$$\epsilon = \left(\max \left\{ \frac{Bs \log\left(\frac{n}{s}\right)}{n}, \frac{B'(1-s)}{n'} \log\left(\frac{n'}{1-s}\right) \right\} \right)^{\frac{q+1}{q+2}} \quad (55)$$

because $\hat{\epsilon} = \epsilon^{2 - \frac{q}{q+1}}$.

Now, we take $f = \hat{f}_{T,T',\phi} \in \mathcal{H}_\tau$ and the above choice of ϵ (55), we have, with probability at least $1 - \delta/2$,

$$\begin{aligned} & \varepsilon(\hat{f}_{T,T',\phi}) - \varepsilon(f_c) - (\varepsilon_{T,T'}(f) - \varepsilon_{T,T'}(f_c)) \\ \stackrel{(49)}{\leq} & 5\epsilon^{1 - \frac{q}{2(q+1)}} \left((\varepsilon(\hat{f}_{T,T',\phi}) - \varepsilon(f_c))^{\frac{q}{q+1}} + \epsilon^{\frac{q}{q+1}} \right)^{1/2} \\ \stackrel{(55)}{=} & 5 \left(\max \left\{ B \frac{s}{n} \log\left(\frac{n}{s}\right), B' \frac{(1-s)}{n'} \log\left(\frac{n'}{1-s}\right) \right\} \right)^{1/2} \\ & \left((\varepsilon(\hat{f}_{T,T',\phi}) - \varepsilon(f_c))^{\frac{q}{q+1}} + \left(\max \left\{ B \frac{s}{n} \log\left(\frac{n}{s}\right), B' \frac{(1-s)}{n'} \log\left(\frac{n'}{1-s}\right) \right\} \right)^{\frac{q}{q+2}} \right)^{1/2} \\ \leq & 5 \left(\max \left\{ B \frac{s}{n} \log\left(\frac{n}{s}\right), B' \frac{(1-s)}{n'} \log\left(\frac{n'}{1-s}\right) \right\} \right)^{1/2} (\varepsilon(\hat{f}_{T,T',\phi}) - \varepsilon(f_c))^{\frac{q}{2(q+1)}} \\ & + 5 \left(\max \left\{ B \frac{s}{n} \log\left(\frac{n}{s}\right), B' \frac{(1-s)}{n'} \log\left(\frac{n'}{1-s}\right) \right\} \right)^{\frac{q+1}{q+2}}. \end{aligned}$$

Here, we have used $\sqrt{a+b} \leq \sqrt{a} + \sqrt{b}$ for all $a, b > 0$ in the last inequality. To further tighten this upper bound, we apply Young's Inequality (39) with

$$a = 5 \left(\max \left\{ B \frac{s}{n} \log\left(\frac{n}{s}\right), B' \frac{(1-s)}{n'} \log\left(\frac{n'}{1-s}\right) \right\} \right)^{1/2}, \quad b = (\varepsilon(\hat{f}_{T,T',\phi}) - \varepsilon(f_c))^{\frac{q}{2(q+1)}}, \quad p = \frac{2(q+1)}{q+2}, \quad p^* = \frac{2(q+1)}{q}$$

and get

$$\begin{aligned}
& 5 \left(\max \left\{ B \frac{s}{n} \log \left(\frac{n}{s} \right), B' \frac{(1-s)}{n'} \log \left(\frac{n'}{1-s} \right) \right\} \right)^{1/2} \left(\varepsilon(\hat{f}_{T,T',\phi}) - \varepsilon(f_c) \right)^{\frac{q}{2(q+1)}} \\
& \leq \frac{\left(5 \left(\max \left\{ B \frac{s}{n} \log \left(\frac{n}{s} \right), B' \frac{(1-s)}{n'} \log \left(\frac{n'}{1-s} \right) \right\} \right)^{1/2} \right)^{\frac{2(q+1)}{q+2}}}{\frac{2(q+1)}{q+2}} + \frac{\varepsilon(\hat{f}_{T,T',\phi}) - \varepsilon(f_c)}{\frac{2(q+1)}{q}} \\
& \leq 5^{\frac{2(q+1)}{q+2}} \left(\max \left\{ B \frac{s}{n} \log \left(\frac{n}{s} \right), B' \frac{(1-s)}{n'} \log \left(\frac{n'}{1-s} \right) \right\} \right)^{\frac{q+1}{q+2}} + \frac{\varepsilon(\hat{f}_{T,T',\phi}) - \varepsilon(f_c)}{2}. \tag{56}
\end{aligned}$$

Furthermore, we have

$$\begin{aligned}
B & \stackrel{(53)}{=} c_q \left(\frac{2c_{\alpha,d}}{2 - \frac{q}{q+1}} m^2 N + \log \left(\frac{4}{\delta} \right) + c_{\alpha,d} m^2 N \log(nmN) \right) \\
& \leq c_q \left(\frac{2c_{\alpha,d}}{2 - \frac{q}{q+1}} + c_{\alpha,d} \right) \left(m^2 N + \log \left(\frac{4}{\delta} \right) + m^2 N \log(nmN) \right) \\
& \leq c_{q,\alpha,d} \left(\log \left(\frac{4}{\delta} \right) + m^2 N (1 + \log(nmN)) \right), \tag{57}
\end{aligned}$$

where $c_{q,\alpha,d} = c_q \left(\frac{2c_{\alpha,d}}{2 - \frac{q}{q+1}} + c_{\alpha,d} \right) \geq 1$ is a positive constant depending only on q, c_0, α , and d . Similarly, we know

$$B' \leq c_{q,\alpha,d} \left(\log \left(\frac{4}{\delta} \right) + m^2 N (1 + \log(n'mN)) \right). \tag{58}$$

Finally, we get with probability at least $1 - \delta/2$,

$$\begin{aligned}
& \varepsilon(\hat{f}_{T,T',\phi}) - \varepsilon(f_c) - (\varepsilon_{T,T'}(f) - \varepsilon_{T,T'}(f_c)) \\
& \stackrel{(56)}{\leq} 5^{\frac{2(q+1)}{q+2}} \left(\max \left\{ B \frac{s}{n} \log \left(\frac{n}{s} \right), B' \frac{(1-s)}{n'} \log \left(\frac{n'}{1-s} \right) \right\} \right)^{\frac{q+1}{q+2}} + \frac{\varepsilon(\hat{f}_{T,T',\phi}) - \varepsilon(f_c)}{2} \\
& \leq 5^{\frac{2(q+1)}{q+2}} (\max\{B, B'\})^{\frac{q+1}{q+2}} \left(\max \left\{ \frac{s}{n} \log \left(\frac{n}{s} \right), \frac{(1-s)}{n'} \log \left(\frac{n'}{1-s} \right) \right\} \right)^{\frac{q+1}{q+2}} \\
& \quad + \frac{\varepsilon(\hat{f}_{T,T',\phi}) - \varepsilon(f_c)}{2} \\
& \stackrel{(57),(58)}{\leq} C_{q,\alpha,d} \left(\log \left(\frac{4}{\delta} \right) + m^2 N (\log(nmN) + \log(n'mN)) \right)^{\frac{q+1}{q+2}} \\
& \quad \cdot \left(\max \left\{ \frac{s}{n} \log \left(\frac{n}{s} \right), \frac{(1-s)}{n'} \log \left(\frac{n'}{1-s} \right) \right\} \right)^{\frac{q+1}{q+2}} + \frac{\varepsilon(\hat{f}_{T,T',\phi}) - \varepsilon(f_c)}{2},
\end{aligned}$$

where $C_{q,\alpha,d}$ is a positive constant depending only on q, c_0, α , and d .

Specifically, if we choose $n' \in \mathbb{N}$ such that $(\frac{1-s}{s})n \leq n' \leq n$, then we get with probability at least $1 - \delta/2$,

$$\begin{aligned}
& \varepsilon(\hat{f}_{T,T',\phi}) - \varepsilon(f_c) - (\varepsilon_{T,T'}(f) - \varepsilon_{T,T'}(f_c)) \\
& \leq C_{q,\alpha,d} \left(\log \left(\frac{4}{\delta} \right) + 2m^2 N \log(nmN) \right)^{\frac{q+1}{q+2}} \left(\frac{s}{n} \log \left(\frac{n}{s} \right) \right)^{\frac{q+1}{q+2}} + \frac{\varepsilon(\hat{f}_{T,T',\phi}) - \varepsilon(f_c)}{2}.
\end{aligned}$$

The proof is complete. \square

C.4 Combining error bounds together

Now that we have derived the upper bounds of the estimation errors and the approximation error, we can combine them together to prove Theorem 4.1.

Proof of Theorem 4.1. We first plug in the upper bounds of the estimation error terms given in Lemma 5 and Lemma 8, respectively. We choose $n \in \mathbb{N}$ such that $\tau \geq \frac{1}{n}$ and $n' \in \mathbb{N}$ such that $(\frac{1-s}{s})n \leq n' \leq n$. With probability at least $1 - \delta$, we have

$$\begin{aligned}
& \varepsilon(\hat{f}_{T,T',\phi}) - \varepsilon(f_c) \\
& \stackrel{(21)}{\leq} \{\varepsilon(\hat{f}_{T,T',\phi}) - \varepsilon_{T,T'}(\hat{f}_{T,T',\phi})\} + \{\varepsilon_{T,T'}(f_{\mathcal{H}}) - \varepsilon(f_{\mathcal{H}})\} + \{\varepsilon(f_{\mathcal{H}}) - \varepsilon(f_c)\} \\
& \stackrel{(37),(48)}{\leq} C_{q,\alpha,d} \left(\log\left(\frac{4}{\delta}\right) + 2m^2 N \log(nmN) \right)^{\frac{q+1}{q+2}} \left(\frac{s}{n} \log\left(\frac{n}{s}\right) \right)^{\frac{q+1}{q+2}} + \frac{\varepsilon(\hat{f}_{T,T',\phi}) - \varepsilon(f_c)}{2} \\
& \quad + C_q \left(\log\left(\frac{4}{\delta}\right) \right) \left(s^{\frac{1}{q+2}} \left(\frac{1}{n} \right)^{\frac{q+1}{q+2}} + (1-s)^{\frac{1}{q+2}} \left(\frac{1}{n'} \right)^{\frac{q+1}{q+2}} \right) \\
& \quad + \frac{(\varepsilon(f_{\mathcal{H}}) - \varepsilon(f_c))}{2} + (\varepsilon(f_{\mathcal{H}}) - \varepsilon(f_c)),
\end{aligned}$$

which implies

$$\begin{aligned}
& \varepsilon(\hat{f}_{T,T',\phi}) - \varepsilon(f_c) \\
& \leq 2C_{q,\alpha,d} \left(\log\left(\frac{4}{\delta}\right) + 2m^2 N \log(nmN) \right)^{\frac{q+1}{q+2}} \left(\frac{s}{n} \log\left(\frac{n}{s}\right) \right)^{\frac{q+1}{q+2}} \\
& \quad + 2C_q \left(\log\left(\frac{4}{\delta}\right) \right) \left(s^{\frac{1}{q+2}} \left(\frac{1}{n} \right)^{\frac{q+1}{q+2}} + (1-s)^{\frac{1}{q+2}} \left(\frac{1}{n'} \right)^{\frac{q+1}{q+2}} \right) + 3(\varepsilon(f_{\mathcal{H}}) - \varepsilon(f_c)). \tag{59}
\end{aligned}$$

For the last term $\varepsilon(f_{\mathcal{H}}) - \varepsilon(f_c)$ (i.e., the approximation error term), we use the upper bound derived in Lemma 3 in (22), which is given by

$$\varepsilon(f_{\mathcal{H}}) - \varepsilon(f_c) \leq 8c_0 (\tau + \|\hat{\eta} - \eta\|_{L^\infty[0,1]^d})^{q+1}.$$

We can take $\hat{\eta} \in \mathcal{H}_\tau$ such that

$$\|\hat{\eta} - \eta\|_{L^\infty[0,1]^d} \leq (2r+1)(1+d^2+\alpha^2)6^d N 2^{-m} + r3^\alpha N^{-\frac{\alpha}{d}}$$

by (20) in Lemma 1. Since $\tau \leq \frac{s}{1-s}$, by choosing $c_{r,\alpha,d} = (2r+1)(1+d^2+\alpha^2)(6^d+3^\alpha)$, we see that

$$\|\hat{\eta} - \eta\|_{L^\infty[0,1]^d} + \tau \leq \frac{s}{1-s} c_{r,\alpha,d} (N 2^{-m} + N^{-\frac{\alpha}{d}}), \tag{60}$$

Then, we have

$$\varepsilon(f_{\mathcal{H}}) - \varepsilon(f_c) \stackrel{(60)}{\leq} 8c_0 \left(\frac{s}{1-s} c_{r,\alpha,d} \right)^{q+1} (N 2^{-m} + N^{-\frac{\alpha}{d}})^{q+1}. \tag{61}$$

Next, we plug in the above upper bound of $\varepsilon(\hat{f}_{\mathcal{H}}) - \varepsilon(f_c)$ in (61) to (59) and get

$$\begin{aligned} \varepsilon(\hat{f}_{T,T',\phi}) - \varepsilon(f_c) &\stackrel{(61)}{\leq} 2C_{q,\alpha,d} \left(\log \left(\frac{4}{\delta} \right) + 2m^2 N \log(nmN) \right)^{\frac{q+1}{q+2}} \left(\frac{s}{n} \log \left(\frac{n}{s} \right) \right)^{\frac{q+1}{q+2}} \\ &\quad + 2C_q \left(\log \left(\frac{4}{\delta} \right) \right) \left(s^{\frac{1}{q+2}} \left(\frac{1}{n} \right)^{\frac{q+1}{q+2}} + (1-s)^{\frac{1}{q+2}} \left(\frac{1}{n'} \right)^{\frac{q+1}{q+2}} \right) \\ &\quad + 24c_0 \left(\frac{s}{1-s} c_{r,\alpha,d} \right)^{q+1} (N2^{-m} + N^{-\frac{\alpha}{d}})^{q+1}. \end{aligned}$$

We choose the smallest $m \in \mathbb{N}$ such that $N2^{-m} \leq N^{-\frac{\alpha}{d}}$, that is

$$m = \left\lceil \left(1 + \frac{\alpha}{d} \right) \frac{\log N}{\log 2} \right\rceil. \quad (62)$$

Then

$$N2^{-m} + N^{-\frac{\alpha}{d}} \leq 2N^{-\frac{\alpha}{d}}. \quad (63)$$

When $n \geq 8^8$, we have $\frac{n}{(\log n)^4} \geq \sqrt{n}$ and thereby

$$N \geq n^{\frac{d}{2(d+\alpha(q+2))}}. \quad (64)$$

So the requirement $N \geq \max\{(\alpha+1)^d, (r+1)e^d\}$ is satisfied when

$$n \geq C_{q,r,\alpha,d} := 8^8 + (\alpha+1)^{2(d+\alpha(q+2))} + (r+1)e^{2(d+\alpha(q+2))}.$$

Let $n \geq C_{q,r,\alpha,d}$. Then $N \leq n$. We also know that $\frac{s}{n} \log \left(\frac{n}{s} \right) \leq \frac{\log n}{n}$. Then, we have

$$\begin{aligned} &\varepsilon(\hat{f}_{T,T',\phi}) - \varepsilon(f_c) \\ &\stackrel{(62),(63)}{\leq} 2C_{q,\alpha,d} \left(\log \left(\frac{4}{\delta} \right) + 2 \left[\left(1 + \frac{\alpha}{d} \right) \frac{\log N}{\log 2} \right]^2 N \log(mn^2) \right)^{\frac{q+1}{q+2}} \left(\frac{\log n}{n} \right)^{\frac{q+1}{q+2}} \\ &\quad + 2C_q \left(\log \left(\frac{4}{\delta} \right) \right) \left(s^{\frac{1}{q+2}} \left(\frac{1}{n} \right)^{\frac{q+1}{q+2}} + (1-s)^{\frac{1}{q+2}} \left(\frac{1}{n'} \right)^{\frac{q+1}{q+2}} \right) \\ &\quad + 24c_0 \left(\frac{s}{1-s} c_{r,\alpha,d} \right)^{q+1} (2N^{-\frac{\alpha}{d}})^{q+1}. \end{aligned}$$

Our choice of N is the smallest integer such that

$$\left(N \frac{(\log n)^4}{n} \right)^{1/(q+2)} \geq N^{-\frac{\alpha}{d}}. \quad (65)$$

Finally, we have, with probability at least $1 - \delta$,

$$\begin{aligned} \varepsilon(\hat{f}_{T,T',\phi}) - \varepsilon(f_c) &\stackrel{(64),(65)}{\leq} C_{q,r,\alpha,d} \left(\frac{s}{1-s}\right)^{q+1} \log\left(\frac{4}{\delta}\right) \left(\frac{n}{(\log n)^4}\right)^{-\frac{d}{d+\alpha(q+2)} \cdot \frac{\alpha(q+1)}{d}} \\ &= C_{q,r,\alpha,d} \left(\frac{s}{1-s}\right)^{q+1} \log\left(\frac{4}{\delta}\right) \left(\frac{n}{(\log n)^4}\right)^{-\frac{\alpha(q+1)}{d+\alpha(q+2)}}, \end{aligned}$$

where $C_{q,r,\alpha,d}$ is a positive constant depending only on q, c_0, r, α , and d . When $3 \leq n \leq C_{q,r,\alpha,d}$, we have

$$\log\left(\frac{4}{\delta}\right) \left(\frac{n}{(\log n)^4}\right)^{-\frac{\alpha(q+1)}{d+\alpha(q+2)}} \geq (C_{q,r,\alpha,d})^{-\frac{\alpha(q+1)}{d+\alpha(q+2)}},$$

so Theorem 1 holds. The proof is complete. □

Appendix D Experimental Details

We proceed to share more details of our experiments for reproducibility and to explain our design choices.

D.1 Dataset Selection

To evaluate and compare our with existing methods, we select two real-world datasets: NSL-KDD [Tavallae et al., 2009] and Kitsune [Mirsky et al., 2018]. NSL-KDD is an updated version of the KDDCup99 dataset [kdd, October 1999] that is used as a common anomaly detection benchmark (e.g., Zhang et al. [2022], Shenkar and Wolf [2022], Qiu et al. [2021], Kim et al. [2020]). It contains four types of attacks as anomalies: Denial of Service (DoS), probe, remote access (RA, also known as remote-to-local (R2L)) and privilege escalation (PE, also known as user-to-root (U2R)) attacks. While this well-established benchmark dataset serves its purpose well for the evaluation, we note that other newer datasets may reflect the current landscape of network attacks better. Hence, we also experiment with the Kitsune dataset, which has more up-to-date data. Similar to NSL-KDD, Kitsune is a network traffic dataset but was created in 2018, by a top security conference work [Mirsky et al., 2018]. This dataset contains two networks: one with 8 types of network attacks and the other with just 1 attack. For a fair comparison across attacks while maintaining diversity, we select the first network with 8 attacks. To be precise, there are 8 datasets, each with normal data and one type of attack. We follow their set-up to use the first 1 million samples as training and the rest for evaluation. During evaluation, we noticed that all models tested consistently obtain random performance for the video injection attack, similar to the sub-par results obtained in the original paper, so we do not include the results from this attack in the paper for brevity. The other seven attacks we use as anomalies can be split into 3 DoS-like attacks (Simple Service Discovery Protocol (SSDP) flood, Secure Socket Layer (SSL) renegotiation and SYN DoS), 2 reconnaissance attacks (Operating System (OS) scan and fuzzing) and 2 man-in-the-middle (MitM) attacks (active wiretap and Address Resolution Protocol (ARP) MitM). We provide a summary of the attacks from the two datasets in Table 4. These two datasets have similar dimensionality — 119 (after one-hot encoding) and 115 for NSL-KDD and Kitsune respectively. This dimensionality is usually considered low in the deep learning literature (where images and text are used, e.g., Kim et al. [2020]), but is high for tabular data (see Qiu et al. [2021], Shenkar and Wolf [2022] for comparisons with other benchmarks on tabular healthcare datasets Thyroid [Quinlan, 1987] and Arrhythmia [Guvenir et al., 1998], and Pang et al.

Table 4: Summary of attacks and examples of potentially indicative features of the attacks.

Dataset	Attack	Description	Potential Features for Detection
NSL-KDD	DoS	Generate a large number of request/response packets to exhaust victims' resources.	Basic TCP connection and traffic features. For example, count, protocol_type, error_rate, error_rate, etc.
	Probe	Send probing packets to gather information about the target system based on the responses.	Basic TCP connection and traffic features. For example, count, service, srv_count, diff_srv_rate, dst_host_same_srv_rate, etc.
	RA	Send packets with vulnerability-exploiting payloads resulting in gaining local access on the host.	Content features. For example, is_guest_login, is_hot_login, logged_in, num_failed_logins, etc.
	PE	Send packets with vulnerability-exploiting payloads resulting in privilege escalation on the host.	Content features. For example, num_root, root_shell, su_attempted, etc.
Kitsune	SSDP Flood	Send a large number of spoofed Simple Service Discovery Protocol (SSDP) packets to Universal Plug and Play (UPnP) devices which generate an overwhelming amount of response packets to the victim.	Bandwidth features. For example, statistics of packet count, size, and jitter.
	SSL Reneg.	Send a large number of SSL renegotiation packets to exhaust servers' resources.	Bandwidth features. For example, statistics of packet count, size, and jitter.
	SYN DoS	Send a large number of SYN packets to exhaust servers' resources.	Bandwidth features. For example, statistics of packet count, size, and jitter.
	Wiretap	Intercept local area network (LAN) traffic via active wiretap (network bridge).	Bandwidth features (indirect). For example, statistics of packet jitter.
	ARP MitM	Intercept LAN traffic via an ARP poisoning attack.	Bandwidth features (indirect). For example, statistics of packet jitter.
	Fuzzing	Send random commands to web servers' Common Gateway Interface (CGI) to find vulnerabilities.	Content features (not explicitly included in the dataset).
	OS Scan	Send selected probe packets to hosts and infer the OS based on responses' fingerprints.	Content features (not explicitly included in the dataset).

[2019] for other common lower-dimensional tabular anomaly datasets). With both datasets, we can test our methodology on real-world scenarios across different times and anomaly types in network traffic.

D.2 Model Choice

Model details can be found in our code implementation. In this section, we outline how we chose certain hyperparameters of certain models.

For classification-based models, as mentioned in the text, it was difficult to systematically validate our choices (e.g., with cross validation) because validation performance was perfect. We use the idea behind structural risk minimization (SRM) to decrease model complexity while validation loss converges to zero. For SVM, we chose to use a high ℓ_2 -regularization for a “simpler” (sparser) model. To choose theory classifier hyperparameters, we also ensure that the model is complex enough by requiring that it converges quickly. Since we repeat experiments thrice, we find the optimal model size (depth and width) that converges within

a couple (1-7) of epochs for the 3 runs, rather than just 1 epoch for all 3 runs.³ We do this by increasing the size of the neural network, and if the number of epochs to converge is within a couple of epochs, we use that neural network; otherwise, we continue increasing the size of the neural network. We chose to start the search with a small width, but not smaller than the data dimensional, to prevent anomalies from projecting onto normal points/regions, as observed in Lau et al. [2024a]. For the NS-NN, the hyperparameters we could choose were the network’s depth, width, and dropout probabilities. We use their proposed configurations as hyperparameters to try. Since they tried three configurations of depth (2/3/4 layers), we increased the width ratio (9.1/27.6/46.1 neurons per dimension per hidden layer)⁴ and dropout (0.34/0.57/0.8) with increasing depth. We report all 3 networks in this Supplement, but we chose the network with 2 layers to report in the main text for the following reason: the deepest had the worst test results and the other 2 had comparable results, so we adopt the SRM approach here too.

For the unsupervised methods, we trained only with normal data. For OCSVM, we chose the default scikit-learn hyperparameters with $\nu = 0.05$. We also tried $\nu \approx 0$ but had much worse results that we do not report. For Isolation Forest, we tried 50/100/150 estimators and observed that the validation performance of normal versus synthetic anomalies were all perfect, so we chose to implement 50 estimators as per SRM. For DeepSVDD, we use the autoencoder architecture with the lowest validation loss during pre-training. We tried with 3 sets of encoder architectures (with the decoder mimicking the reverse): d -90-45-20, d -90-45, d -60-20 (d is 119 for NSL-KDD and 115 for Kitsune).

D.3 Full Results

We report full results for NSL-KDD in Table 5 (less the ablation results in Section 5.4) and Kitsune in Table 6. Since the results for NSL-KDD were elaborated on in the ablations in Section 5.4, we focus on Kitsune (Table 6). For our theory classifier, we used $D = 4$ layers and varied the width w to control the complexity of the model (as detailed in the previous section), but report results for all models as an ablation on the width w . We underline the results that were ultimately used for our theory classifier and report results in bold for the best theory classifier. In Table 6, We notice that our method of choosing hyperparameters is the best (when the result is underlined and in bold) 5/7 times. The outlier is for SSL renegotiation attacks, when the best theory classifier scored a much higher AUPR than the other methods as well. Overall, wider models generally work better for easier attacks (SSDP and SSL, less SYN) and narrower models generally work better for harder attacks (wiretap, ARP MitM and OS scan, less fuzzing). More exploration can be done here on other datasets too.

³If it is too time-consuming, some discretion can be taken to relax this requirement. We observe that results generally do not vary too much if this condition is relaxed slightly.

⁴We obtained the width ratio by taking the width used for the original dataset divided by the dataset dimensionality. The width we use is the width ratio multiplied by our dataset dimensionality. Using the width ratio allows us to calibrate the relative width, especially because the data Sipple [2020] used had much lower (< 40) dimensionality than our datasets.

Table 5: AUPR for KDD, split across attacks in each column. Higher is better. Suffix for NS-NN refers to the number of layers.

Model\Attack	DoS	Probe	RA	PE	
Random	0.431	0.197	0.007	0.218	
Classify	SVM	0.891±0.001	0.838±0.000	0.014±0.000	0.320±0.001
	TC (Ours)	0.909±0.001	0.943±0.002	0.030±0.008	0.401±0.017
	NS-NN2	0.517±0.056	0.223±0.040	0.009±0.000	0.217±0.000
	NS-NN3	0.669±0.097	0.411±0.062	0.009±0.000	0.217±0.000
	NS-NN4	0.431±0.000	0.197±0.000	0.009±0.000	0.217±0.000
Unsup.	OCSVM	0.891±0.000	0.834±0.001	0.018±0.000	0.356±0.000
	IsoF	0.945±0.005	0.941±0.015	0.046±0.039	0.398±0.039
	DeepSVDD	0.824±0.003	0.756±0.003	0.031±0.000	0.492±0.005

Table 6: AUPR for Kitsune, split across attack types. Width w in parentheses for our theory classifier (TC). Underlined results are the results from the models used. Results reported in bold represent the best of the category or results that are within 1 standard deviation of the best. We do not report results in bold for NS-NN because the results are roughly the same.

Model	SSDP	SSL	SYN	Wiretap	ARP MitM	Fuzzing	OS Scan		
Random	0.468	0.077	0.004	0.217	0.761	0.348	0.094		
Classify	SVM	1.000±0.000	0.678±0.001	0.060±0.006	0.539±0.005	0.724±0.017	0.322±0.007	0.576±0.000	
	TC (115)	0.999±0.000	0.631±0.012	0.265±0.026	0.747±0.084	0.832±0.105	0.368±0.007	0.501±0.000	
	TC (335)	0.998±0.002	0.565±0.179	0.246±0.002	0.743±0.133	0.851±0.099	0.535±0.001	0.495±0.009	
	TC (500)	0.999±0.002	0.574±0.164	0.167±0.141	0.666±0.061	0.820±0.111	0.693±0.139	0.393±0.176	
	TC (678)	0.999±0.001	0.768±0.049	0.189±0.123	0.631±0.045	0.810±0.051	0.606±0.105	0.498±0.006	
	NS-NN2	0.999±0.000	0.649±0.002	0.242±0.000	0.723±0.000	0.801±0.010	0.360±0.000	0.500±0.001	
	NS-NN3	0.993±0.003	0.563±0.009	0.221±0.028	0.722±0.000	0.761±0.000	0.360±0.000	0.500±0.000	
	NS-NN4	0.994±0.002	0.548±0.009	0.111±0.078	0.722±0.000	0.761±0.000	0.353±0.005	0.501±0.000	
	Unsup.	OCSVM	0.999±0.000	0.640±0.000	0.248±0.000	0.571±0.000	0.766±0.000	0.299±0.000	0.500±0.000
		IsoF	0.995±0.007	0.489±0.007	0.229±0.018	0.691±0.013	0.651±0.012	0.254±0.010	0.502±0.001
DeepSVDD		0.998±0.000	0.640±0.000	0.237±0.001	0.627±0.002	0.620±0.001	0.267±0.006	0.500±0.000	